Fast calcium wave propagation mediated by electrically conducted excitation and boosted by CICR

J.M.A.M. Kusters[*], W.P.M. van Meerwijk[$],
D.L.Ypey[$], A.P.R. Theuvenet[$] and C.C.A.M. Gielen[*]

[*]Dept. of Biophysics, Radboud University Nijmegen,
Geert Grooteplein 21, 6525 EZ Nijmegen, The Netherlands
[$]Dept. of Cell Biology, Radboud University Nijmegen,
Toernooiveld 1, 6525 ED Nijmegen, The Netherlands

Corresponding author: C.C.A.M. Gielen,
Dept. of Biophysics,
Radboud University Nijmegen,
Geert Grooteplein 21,
6525 EZ Nijmegen, The Netherlands,
email: s.gielen@science.ru.nl,
tel: +31-24-3614244 , fax: +31-24-3541435

Abstract

We have investigated synchronization and propagation of calcium oscillations, mediated by gap junctional excitation transmission. For that purpose we used an experimentally based model of normal rat kidney (NRK) cells, electrically coupled in a 1-dimensional configuration (linear strand). Fibroblasts such as NRK cells, can form an excitable syncytium and generate spontaneous inositol 1,4,5-triphosphate (IP_3) mediated intracellular calcium waves, which may spread over a monolayer culture in a coordinated fashion.

An intracellular calcium oscillation in a pacemaker cell causes a membrane depolarization from within that cell via Cl(Ca)-channels leading to a L-type Ca-channel based action potential in that cell. This action potential is then transmitted to the electrically connected neighbor cell and the calcium inflow during that transmitted action potential triggers a calcium wave in that neighbor cell by opening of IP_3-receptor channels, causing calcium induced calcium release (CICR). In this way the calcium wave of the pacemaker cell is rapidly propagated by the electrically transmitted action potential. Propagation of action potentials in a strand of cells depends on the number of terminal pacemaker cells, on the G_{CaL} conductance of the cells, and on the electric coupling between the cells. Our results show that the coupling between IP_3-mediated calcium oscillations and action potential firing provides a robust mechanism for fast propagation of activity across a network of cells, which is representative for many other cell types such as gastrointestinal cells, urethral cells and pacemaker cells in the heart.

Key words: gap junctions; calcium waves; pacemaking; electrical coupling; action potential propagation; IP_3-receptor; NRK cell

Introduction

Intracellular calcium oscillations are very common and have been reported in a large variety of cell types, such as smooth muscle cells (39), hepatocytes (47), oocytes (5), normal rat kidney fibroblast cells (16) and pancreatic acinar cells (11,33). In these cell types the cytosolic calcium transients are evoked by inositol 1,4,5-triphosphate (IP_3)-linked agonist stimulation: after interacting with cell-surface receptors, agonists activate phospholipase C (PLC) and induce the release of IP_3. IP_3 then triggers calcium release from intracellular stores through IP_3- sensitive calcium release channels in the ER membrane (32). Calcium liberation from the endoplasmic reticulum (ER) can also be activated by cytosolic calcium in the presence of IP_3. In our model, the main mechanism of calcium-induced calcium-release (CICR) is the opening of the IP_3-receptor (but other release mechanisms of intracellular calcium may do as well).

In the cell types mentioned above, the cells are connected by gap junctions, allowing diffusion of IP_3 and calcium. Since both IP_3 and calcium facilitate intracellular calcium oscillations, diffusion of calcium and IP_3 through the gap junctions could provide an effective way for synchronization of intracellular calcium oscillations in neighboring cells and for propagation of waves of intracellular calcium oscillations through the network (see e.g. 10, 19, 20, 40). The propagation of calcium waves through the network has been the topic of many studies, but the cellular mechanisms involved in the propagation of calcium oscillations can be very different. Most studies refer to the propagation of calcium waves in non-excitable cells with intracellular IP_3-mediated calcium oscillations, where oscillations in cells are coupled by diffusion of IP_3 and calcium through gap junctions (see e.g. 12, 19, 20, 43). In our study we will ignore coupling of oscillations by calcium and IP_3 diffusion for good reasons which will be explained in the Discussion section.

At the other hand, there is propagation of electrical activity in networks of cells electrically coupled by gap junctions, such as in the ventricular myocardium (17, 18, 23 - 26). In such types of cell networks, propagation of electrical activity is the result of depolarization of a cell by action potential firing of its neighbor. For adequate gap-junctional coupling, an action potential causes a depolarization in neighboring cells, which opens their membrane channels and so triggers an action potential.

Some recent studies have focused on cell types which have both IP_3-mediated calcium oscillations and action potentials, such as in interstitial cells of Cajal (4), sinoatrial nodal cells in the heart (31), lymphatic smooth muscle cells (22) and in NRK fibroblasts (27). These cell types have the interesting property that the mechanisms of IP_3-mediated calcium oscillation and action potential generation are coupled, and interact with each other (28). An action potential can trigger a calcium transient since inflow of calcium during an action potential causes CICR. In the other direction, the increase of cytosolic calcium due to release of calcium through the IP_3-receptor opens calcium-dependent channels in the membrane causing a depolarization. In NRK-cells the major calcium-dependent membrane channel type is the calcium-dependent chloride channel with a Nernst potential near -20 mV. This depolarization may then trigger an action potential (6, 27). Since electrical coupling through gap junctions is faster than chemical coupling by diffusion of calcium and IP_3 through gap junctions (6, 36), the intracellular calcium oscillations between cells are also (indirectly) coupled by the electrical coupling by gap junctions.

Because of the positive interaction between the IP_3-mediated calcium oscillator and membrane depolarization, excitable cells with IP_3-mediated calcium oscillations may be very robust pacemakers for propagating activity in the network (45). Recently, Imtiaz et al. (22) have investigated the various coupling modes of two cells with different amounts of IP_3 and, therefore, different intrinsic oscillation frequencies. These authors showed that the chemical

and electrical coupling by gap junctions can cause anti-phase or in-phase oscillations of the cell pair, depending on the amount of IP_3. Moreover, these authors showed that weak coupling (small conductance of the gap junction) is sufficient to synchronize heterogeneous cell pairs.

Following up on the study by Imtiaz et al. (22) on a pair of cells, we have investigated the initiation and propagation of activity in a network with excitable cells with IP_3-mediated calcium oscillators by gap junctional coupling. Imtiaz et al. (22) have shown that a pacemaker cell can drive the calcium oscillations in a neighboring cell with a lower IP_3 concentration and a correspondingly lower intrinsic oscillation frequency. The question that we will address is: "What happens when more cells with a low IP_3 concentration are coupled to this single pacemaker.?" And what happens if a pacemaker is coupled to cells which do not have an intrinsic oscillation frequency, because the IP_3-concentration is too small? If that number of coupled follower cells increases, the current from the pacemaker cell to the follower cells will spread through the whole network. When the gap-junctional conductance is very small, the current might be too small to depolarize the neighboring cells. However, when the gap-junctional conductance is very large, current will spread throughout the network and, if the network is large, the net current into a neighboring cell may also be too small to depolarize the cell. Therefore, in agreement with previous studies on excitable cells without intracellular calcium oscillations (36), we expect an optimal range of gap-junctional conductances for initiation and propagation of activity in the network. Because of the positive, reinforcing coupling between the intracellular calcium oscillator and the membrane depolarization, we hypothesize that propagation is more robust in excitable cells with both mechanisms compared to cells that lack one of the two.

We addressed these problems using an experimentally verified model for NRK fibroblast cells (27). Contrary to Imtiaz et al. (22) we did not include voltage-dependent IP_3

synthesis. The coupling between cells in our study is by electrical current through the gap junctions. In each individual cell, the electrical phenomena are coupled to the intracellular calcium oscillators by the calcium inflow through the L-type Ca-channels and by calcium inflow through the IP_3-receptor. In the discussion we will evaluate the consequences of this simplification on the propagation of activity.

Model description

In previous studies we have reported a mathematical model of normal rat kidney (NRK) fibroblasts capturing the basic characteristics (27, 28) based on single-cell data (14). This model was obtained by implementation of the dynamics of the membrane ion channels and that of the intracellular calcium oscillator. As an emergent property, the model correctly reproduced the properties of calcium transients, calcium action potentials and the coupling between calcium transients and calcium action potentials.

The model contains two compartments for each cell: the cytosol and the ER. The plasma membrane contains a PMCA, L-type Ca channels, Calcium dependent chloride channels, a nonspecific leak and inward rectifying K channels (Harks et al 2003). The ER membrane contains a SERCA pump, a Calcium leak and an IP_3 receptor channel. Cells are electrically coupled by gap junctions.

The key idea of the model (27) is that auto- and paracrine production of hormones such as PGF2α leads to the production of IP_3, which gives rise to IP_3-mediated intracellular Ca^{2+}-oscillations. These IP_3-mediated calcium oscillations cause periodic calcium transients, which open the Ca^{2+}-dependent Cl-channels ($Cl^-(Ca^{2+})$-channels). These $Cl^-(Ca^{2+})$-channels depolarize the membrane towards the chloride Nernst potential near -20 mV thereby causing activation of the L-type Ca-channels. Opening of calcium channels generates an influx of calcium in the cells with a concomitant further depolarization towards the equilibrium potential for Ca^{2+} -ions. The $Cl^-(Ca^{2+})$-channels remain activated as long as the intracellular Ca^{2+}-level is elevated, resulting in a plateau phase at the chloride Nernst potential at -20 mV. Upon extrusion of Ca^{2+} from the cytoplasm, the $Cl^-(Ca^{2+})$-channels become deactivated, and the cells subsequently repolarize to –70 mV as a result of the activity of inward rectifier K^+-channels (14). Just the other way around, calcium action potentials induce Ca^{2+}-induced Ca^{2+} release (CICR) through the IP_3-receptors.

The autonomous cell oscillator

The NRK cell model by Kusters et al. (27) to describe the dynamics of the cell has two major components: an IP_3-mediated intracellular calcium oscillator and an electrically excitable membrane. Here we describe the main properties of the NRK cell. For more details, we refer to (27).

Calcium in the cytosol plays a key role in coupling the dynamics of the IP_3-mediated calcium oscillator and the cell membrane (28). The rate of change in the membrane potential due to the currents through inward rectifier potassium channels (I_{Kir}), L-type Ca-channels (I_{CaL}), Ca-dependent Cl-channels ($I_{Cl(Ca)}$), leak channels (I_{lk}), and store dependent calcium (SDC)-channels (I_{SDC}) is given by

$$C_m \frac{dV_m}{dt} = -\left(I_{Kir} + I_{lk} + I_{CaL} + I_{Cl(Ca)} + I_{SDC}\right) \qquad \text{(A.1)}$$

I_{Kir} and I_{lk} determine the membrane potential of the cell at rest near -70 mV and are specified by Equations A.2-A.6 in the Appendix.

In NRK cells, the crucial coupling between electrical events at the excitable membrane and the internal calcium oscillations is controlled by the L-type Ca-channel and the calcium-dependent chloride channel. The current through the L-type Ca-channels is given by

$$I_{CaL} = mhG_{CaL}(V_m - E_{CaL}) \qquad \text{(A.7)}$$

where V_m refers to the membrane potential and E_{CaL} refers to the Nernst potential of Ca^{2+} near 50 mV. The L-type Ca-channel has an activation (m), and inactivation (h) variable. The dynamics of m and h obey a first order differential equation with steady-state values m_∞ and h_∞ given by Eqs. A.8 and A.10, respectively, and with time constants given by Eqs. A.9 and A.11.

The current through the Ca-dependent Cl-channel (Cl(Ca)) is given by

$$I_{Cl(Ca)} = \frac{\left[Ca_{cyt}^{2+}\right]}{\left[Ca_{cyt}^{2+}\right] + K_{Cl(Ca)}} G_{Cl(Ca)} \left(V_m - E_{Cl(Ca)}\right) \qquad \text{(A.12)}$$

In addition, the cell membrane has a store-dependent calcium channel (SDC). The conductance of the SDC is inversely related to the calcium concentration in the ER.

$$I_{SDC} = \frac{K_{SDC}}{\left[Ca_{cyt}^{2+}\right] + K_{SDC}} G_{SDC} \left(V_m - E_{SDC}\right) \qquad \text{(A.13)}$$

One of the mechanisms for calcium extrusion from the cytosol is the plasma membrane calcium ATPase (PMCA) pump. The flux of Ca2+-ions through the PMCA pump is described by

$$J_{PMCA} = J_{PMCA}^{\max} \frac{\left[Ca_{cyt}^{2+}\right]}{\left[Ca_{cyt}^{2+}\right] + K_{PMCA}} \qquad \text{(A.16)}$$

Any changes in the cytosolic calcium concentration [Ca^{2+}] are due to buffering of calcium (Eq. A.14), to a net flux of calcium through the plasma membrane (J_{PM}, Eq. A.15), and net fluxes through the ER membrane (Eq. A.18). The latter has a constant leak of calcium J_{lkER} (Eq. A.19), a flux through the IP_3-receptor (J_{IP3R}, Eq. A.20) and active transport of calcium into the ER by the sarcoplasmic/endoplasmic reticulum Ca-ATPase (SERCA) pump (J_{SERCA}, Eq. A.24).

The intracellular calcium oscillator is controlled by the intracellular IP_3-concentration which activates the IP_3-receptor. The flux of Ca^{2+}-ions through the IP_3-channel is described by a Hodgkin-Huxley type formalism

$$J_{IP_3R} = f_\infty^3 w^3 K_{IP_3R} \left(\left[Ca_{ER}^{2+}\right] - \left[Ca_{cyt}^{2+}\right]\right) \qquad \text{(A.20)}$$

with activation variable f and inactivation variable w with the steady state values f_∞ and w_∞ given by Eqs. A.21 and A.22. The time constant for the activation parameter f is considered to be small relative to that of the other processes in the cell. Therefore, we use f_∞ instead of f. The time constant τ_w for the inactivation gate is described by Eq. A.23. This results into

periodic oscillations of calcium flow out of the endoplasmic reticulum (ER) into the cytosol and calcium re-uptake in the ER by activity of the SERCA pump. As suggested by Dupont and Goldbeter (28), the flux of Ca2+-ions through the SERCA pump is described by

$$J_{SERCAA} = J_{SERCA}^{\max} \frac{\left[Ca_{cyt}^{2+}\right]}{\left[Ca_{cyt}^{2+}\right] + K_{SERCA}} \qquad \text{(A.24)}$$

The elevated calcium concentration in the cytosol by opening of the IP_3-receptor activates the Ca-dependent Cl-channels (see Eq. A.12), which depolarize the cell membrane to the Cl^- Nernst potential near -20 mV. As explained by Kusters et al. (27), this depolarization can open the L-type Ca-channels. Opening of the L-type Ca-channels gives rise to a further increase in $\left[Ca_{cyt}^{2+}\right]$. As a result an action potential (AP) with a plateau phase near -20 mV occurs. Calcium in the cytosol is reduced by re-uptake of calcium in the ER by the SERCA and PMCA pump. When the calcium concentration in the cytosol has been restored to its basal level, the Ca-dependent Cl-channels close and the membrane potential repolarizes to the rest potential near -70 mV.

Parameter modification

The full set of equations describing the dynamics and the parameter values of this NRK-model can be found in Kusters et al. (27). In the present model study we had to adjust some parameter values. When calcium in the external medium of NRK cells is replaced by strontium, AP propagation in experiments is more robust (6). The reason is that strontium does not inactivate the L-type Ca-channels as calcium does (14). Since many experimental data were obtained using strontium instead of calcium (6, 7, 14), we omitted the calcium-dependent inactivation factor v_{Ca} in the model equation for the L-type Ca-channel. Another effect is that the current through the L-type Ca-channel is much larger for strontium than for calcium, which is why we have used a larger value for the L-type Ca-channel conductance

G_{CaL} (1.6 nS instead of 0.7 nS). Since the L-type Ca-channel, Ca-dependent Cl-channel and IP_3-receptor are important channels for AP propagation and since activation of these channels was rather small in our old model (27), we changed the following parameters: τ_h (time constant for inactivation of the L-type Ca-channel) a factor 2 longer, τ_m (time constant for activation of the L-type Ca-channel) a factor 2 smaller, the membrane potential for half-maximal activation of m_∞ is set to −10 mV, $K_{Cl(Ca)}$ set to 18 μM, J_{PMCA} set to 3×10^{-5} $\mu mol/(s\times dm^2)$ and G_{lk} set to 0.058 nS. These changes lie within the range of values from experimental observations. The k_{on} and k_{off} parameters of the buffer are set to 1. Table 1 shows the modified parameter values.

Electrical coupling through gap junctions

Many fibroblastic cell types in culture, including NRK cells, are electrically coupled by gap-junctional channels, e.g. composed of connexin43 (Cx43) subunits with a typical conductance between the cell and its surrounding network near 20 nS (13). The monolayer of NRK cells can be approximated by a hexagonal grid (42). Therefore, the total gap-junctional conductance of 20 nS for a cell corresponds to a gap-junctional conductance G_g between two neighboring cells of 20/6 ~ 3 nS, which is in agreement with other experimental data for gap junction coupling between cells where Cx43 subunits are involved (3, 41).

The electrical current flowing through the gap junctions between cell i and other cells in the network was incorporated by an extra term at the right-hand side of Eq. A.1, which resulted in

$$C_m \frac{dV_m}{dt} = -\left(I_{Kir} + I_{lk} + I_{CaL} + I_{Cl(Ca)} + I_{SDC} + \sum_{j\in neighbor\ i} I_{gap}^{ij} \right) \qquad (1)$$

$$I_{gap}^{ij} = G_g \left(V_m^i - V_m^j \right) \qquad (2)$$

where G_g is the conductance of the gap-junction coupling between neighboring cells i and j.

We modeled the AP propagation by electrical coupling of a single pacemaker cell to

surrounding follower cells in a one-dimensional strand (cable). Our aim is to understand the electrical load upon the single pacemaker cell due to coupling to surrounding cells. Fig. 1A shows the equivalent electrical circuit for the passive electrical properties of a one-dimensional strand of follower cells driven by a pacemaker cell ("P"). Each follower cell is represented by a capacitance C and resistance R_f and cells are coupled by the gap-junctional resistance R_g. This passive model is a good approximation as long as the membrane potential does not reach the threshold for action potential firing.

Expanding a network of n follower cells with an additional follower cell (Fig. 1B) gives a relation between Z_n and Z_{n+1}, where Z_n and Z_{n+1} represent the equivalent impedance for an array with n and n+1 follower cells, respectively. This relation is given by

$$Z_{n+1}(\omega) = \frac{Z_{cell}(\omega)\left(R_g + Z_n(\omega)\right)}{R_g + Z_n(\omega) + Z_{cell}(\omega)} \tag{3}$$

where $Z_{cell}(\omega)$ is the impedance of a follower cell in the frequency domain, given by

$$Z_{cell}(\omega) = \frac{R_f}{1+\omega^2\tau_f^2} - i\frac{R_f\omega\tau_f}{1+\omega^2\tau_f^2} \tag{4}$$

with capacitance (C), resistance (R_f) and the characteristic time constant $\tau_f = R_fC$. The equivalent resistance of an infinitely long one-dimensional strand can be calculated by setting $Z_{n+1}(\omega) = Z_n(\omega)$, which gives

$$Z_\infty = \frac{-R_g + \sqrt{\left(R_g^2 + 4Z_{cell}(\omega)R_g\right)}}{2} \tag{5}$$

For an infinitely large strand of cells the net current to the first follower cell (see Fig. 1C) is given by

$$I_{cell} = V_p \frac{Z_\infty}{Z_\infty Z_{cell} + \left(Z_\infty + Z_{cell}\right)\left(R_g + Z_p\right)} = \tag{6}$$

$$V_p \frac{-R_g + \sqrt{\left(R_g^2 + 4Z_{cell}(\omega)R_g\right)}}{-R_g + \sqrt{\left(R_g^2 + 4Z_{cell}(\omega)R_g\right)}Z_{cell} + \left(-R_g + \sqrt{\left(R_g^2 + 4Z_{cell}(\omega)R_g\right)} + 2Z_{cell}\right)\left(R_g + Z_p\right)}$$

From Eqs. 5-6 it is easy to see that I_{cell} becomes zero for infinitely small values of R_g. If R_g becomes infinitely small, $Z\infty$ becomes zero and therefore I_{cell} becomes zero. Eq. 6 shows that I_{cell} is also zero for large values of R_g ($R_g \uparrow \infty$, $I_{cell} = 0$). The optimal value of R_g is found by solving $\frac{\partial I_{cell}}{\partial R_g} = 0$. For the parameter values in our study the optimal value for R_g is about 2.0 10^9 Ohm (G_g = 0.5 nS).

Results

Phase response curves for current pulse and calcium pulse

Understanding the response of a single cell to a current pulse or injection of calcium ions is helpful to understand the interaction between two cells (49). Current and calcium perturbations allow us to determine the Phase Response Curve (PRC), which gives the phase shift ($\Delta\varphi$) of the action potential or calcium oscillator of a NRK pacemaker cell with intrinsic cycle length (T) as a function of the phase (φ) at which the external input is given. When a current pulse of sufficient amplitude is injected into a cell, the elevated membrane potential results in opening of the L-type Ca-channels and, possibly, into action potential firing. The inflow of calcium causes calcium-induced calcium release through the IP_3-receptor channel and gives rise to a phase advance of the IP_3-mediated calcium oscillator. At the other hand, a calcium injection gives rise to a phase advance of the IP_3-mediated calcium oscillator and corresponding Ca^{2+} transient. The resulting depolarization by the Ca-dependent Cl^--channels then leads to advanced appearance of the next action potential (AP).

The phase response curve (PRC) is measured by delivering a precisely timed perturbation and measuring the change in the running cycle duration. The upstroke of the preceding pacemaker action potential is chosen as the reference point (phase zero), since it is very sharp compared to the onset of calcium oscillations (CaOs). Moreover, CaOs change in shape and size. Phase φ is defined by $\varphi = t_p/T$, where t_p is the time when the stimulus is applied, relative to the reference point, and $\Delta\varphi$ is defined as $(T - T_{new})/T$ where T_{new} is the time of occurrence of the following action potential or calcium transient relative to the reference point, i.e. the new cycle length. The PRC quantifies the effect of an input pulse at a given phase on the occurrence of the following action potential or calcium transient. If an input pulse does not affect the next AP or calcium transient, T is unchanged and the phase change $\Delta\varphi$ at that point of the curve is zero. If the input pulse delays the next AP or calcium

transient, $T_{new} > T$ and the phase change $\Delta\varphi$ has a negative value (not observed in our simulations). If the pulse advances the next AP, $T_{new} < T$ and $\Delta\varphi$ is positive. Fig. 2 shows PRCs (lower panels) generated by injecting a depolarizing current pulse with a 50 ms duration of 10, 15 and 20 pA (A) and a calcium pulse associated with a calcium current injection of 1, 2 and 5 pA for 50 ms (B). The top three subpanels in Fig. 2 show an example of the effect of current (15 pA in panels A) and calcium pulses (1 pA in panels B) on the phase advance of the AP and CaO, respectively, (dashed lines) and the unperturbed response (solid lines). The lower panels of A and B show the phase change of the IP_3- mediated calcium oscillator as a function of the timing of the current pulse in the cycle of the calcium oscillator. The lower-left panel shows that a current pulse of 10 pA has no effect on the IP_3-mediated calcium oscillator irrespective of the phase in the action potential cycle (thick solid line). Depolarizing current pulses of 15 pA (dashed-dotted line) and 20 pA (thin solid line) injected at phase $\varphi > 0.2$ trigger the next calcium transient almost immediately via an evoked action potential. Injection at phase $\varphi < 0.1$ has no effect on the next calcium transient, because this period includes the action potential and its refractory period (see Fig. 2A). Note, that these current injections are smaller than the current inflow in the cell by the membrane during an action potential, which is about 25 pA. Fig. 2B shows the phase change of the AP as a function of the phase of the calcium pulse. The figure shows that the phase of the AP does not change for calcium pulses of 1 (thick solid line), 2 (dashed-dotted line) and 5 (thin solid line) pA at phases $\varphi < 0.6$, $\varphi < 0.4$ and $\varphi < 0.3$, respectively. The phase is maximally advanced for $\varphi > 0.7$, $\varphi > 0.5$ and $\varphi > 0.4$, respectively, when triggered by calcium pulses of 5, 2 and 1 pA, respectively. These calcium injections are small relative to the total inflow of calcium from the ER during a calcium transient (approximately 35×10^{-6} μmol) and through the membrane during an action potential (approximately 100×10^{-6} μmol).

The dashed lines plotted in the lower panels in Fig. 2 do not exactly represent the

transitions of the phase changes, but represent interpolations between subsequent points of the PRC curves for steps of 0.1. The PRC's in Fig. 2 show that an intracellular calcium oscillation and an action potential are both capable of triggering an action potential or calcium transient, respectively, except when they occur shortly after a preceding action potential.

Entrainment of Ca-oscillations of two cells by electrical coupling

Since IP_3-mediated calcium oscillations and action potential generation within a cell are tightly coupled processes (Fig 2), electrical coupling between cells by gap junctions provides an indirect (electrical) coupling mechanism between IP_3-mediated calcium oscillations in two neighboring cells. In order to investigate the role of gap junctions in the coupling of IP_3-mediated calcium oscillations of two neighboring cells, we have investigated the entrainment of two pacemaker cells with different intrinsic frequencies (due to different IP_3 concentrations) as a function of gap-junctional conductance.

Fig. 3 shows the major family of entrainment regions, commonly called Arnold tongues (36) (solid lines), as a function of the electrical coupling G_g. Notice that the vertical scale is in pS. The entrainment regions are labeled by the ratio of the frequencies of the CaOs of both cells ($f_2([IP_{3(cell2)}]) / f_1([IP_{3(cell1)}])$). The IP_3 concentration of cell 1 is set to a value of 1.0 μM (this value causes CaOs at intermediate frequencies (f_1 = 1/100 Hz)), while the IP_3 concentration of cell 2 is varied in steps of 0.005 μM at a rate of one step per 9000 seconds from 0.0 μM to 8.0 μM.

When two pacemaker cells are uncoupled ($G_g = 0$), the cells can only have (subharmonic) m/n frequency entrainment when the frequencies f_1 of cell 1 and f_2 of cell 2 are related by $m f_1 = n f_2$ (n and m integers). When the gap-junctional conductance G_g increases in small steps, various modes of entrainment develop before complete synchrony (1:1 entrainment) is established. The value of G_g, where 1:1 entrainment develops, depends on the

difference of the oscillation frequencies of the two cells in the uncoupled mode. The regions, where entrainment takes place, are related by the relation $0 \leq | m f_1 - n f_2 | < \varepsilon(G_g, m, n)$, where ε increases for larger values of G_g. Figure 3 shows only the regions for the major entrainment ratio's for f_2:f_1 (1:2, 2:3, 1:1, 4:3 and 3:2), but in between there are many, much smaller, regions with other ratios of m:n entrainment. The regions for various modes of entrainment grow with G_g and merge until a value of G_g is reached which gives 1:1 entrainment for all frequencies. For example, when we start at G_g = 35 pS and [IP_3] = 0.4 μM for cell 2 (corresponding to an intrinsic oscillation frequency f_2 = 1/190 Hz for the cell in isolation), simulations reveal that this cell exhibits calcium transients at half the frequency of the CaOs in cell 1. For increasing values of [IP_3] in cell 2 at G_g = 35 pS (horizontal dashed line), the following major entrainment regions are observed, 1:2, 2:3, 1:1, 4:3 and 3:2, respectively. In between there are many, much smaller regions with other ratios of m:n entrainment. Fig. 3 predicts that electrical coupling near 60 pS or higher between two cells with one cell having an IP_3 concentration of 1.0 μM is sufficient to completely synchronize two heterogeneous NRK cells, irrespective of the IP_3 concentration in the second cell. In this range (for gap-junctional conductance values above approximately 60 pS) the cell with the lowest oscillation frequency locks to the cell with the highest oscillation frequency. Therefore, in the 1:1 entrainment region left from the ratio f_2/f_1 = 1.0, the frequency of the CaOs is determined by the reference frequency f_1 and on the right side by the variable frequency f_2.

From the results shown in Fig. 3 we infer that under conditions of a physiological gap-junctional coupling strength of 3 nS between NRK cells (13), the intracellular CaOs and APs of two oscillating NRK cells are fully synchronized. The fact that the fastest frequency always determines the synchronized frequency indicates that both calcium oscillators synchronize by phase resetting AP effects and not by continuous interaction (46, 49)

Synchronization of cells in a strand by electrical coupling

To explore the excitation of follower cells by pacemaker cells, we have studied entrainment of a strand of follower cells by a terminal pacemaker cell. Since gap junctions allow diffusion of IP_3, and because follower cells may be subject to stimulation of subthreshold IP_3 production, we assumed nonzero concentrations of IP_3 in the follower cells. For most simulations in this study, the follower cells have an IP_3 concentration of 0.1 μM, which does not give rise to spontaneous Ca-oscillations. For the pacemaker cell we chose an IP_3 concentration of 1.0 μM, which causes spontaneous calcium transients and APs (27).

Fig. 4 shows the results of such an entrainment simulation. The solid and dashed lines demarcate different entrainment regions for a one-dimensional strand of follower cells with $[IP_3]$ = 0.1 and 0.0 μM, respectively, by a single terminal pacemaker cell ($[IP_3]$ = 1.0 μM) as a function of the number of cells and gap-junctional conductance (G_g). Fig. 4 shows that the mode of entrainment depends both on the number of follower cells in the strand as well as on gap-junctional conductance. For a single pacemaker cell and one follower cell ($[IP_3]$ = 0.1 μM), the minimal gap-junctional conductance for full 1:1 entrainment is approximately 0.06 nS. Increasing the number of cells for a fixed value for G_g at 0.1 nS, changes the 1:1 18 entrainment to 1:2 entrainment for 3 cells, to 1:4 entrainment for 4 cells. For 5 or more cells no synchronization takes place anymore when G_g = 0.1 nS. Coupling in the range between 0.25 nS and 0.45 nS is sufficient for complete 1:1 synchronization of CaOs and APs in a one-dimensional network of NRK cells with this IP_3 level, independent of the network size. If the IP_3 concentration in the follower cells is set to 0.0 μM, the same results are obtained for these small values of G_g (dashed lines, super imposed on solid lines). Notice that experimental observations (13) report a gap-junctional conductance for NRK cells of 3 nS, which is much larger than the optimal coupling range in our simulations (0.25-0.45 nS). We will come back to this in the Discussion section.

The entrainment regions are different for a strand of follower cells with IP_3 concentration of 0.1 μM (solid lines) and for a strand with cells set to 0 μM (dashed lines) for G_g values above 0.4 nS. For [IP_3] = 0.1 μM in the follower cells the entrainment changes from 1:2 to 1:3 and 1:4 for increasing values of G_g when the number of follower cells is larger than approximately 20 (solid line). For [IP_3] = 0 the IP_3-receptor in the follower cell is closed and AP transmission fails for G_g above 0.8 nS when the number of cells exceeds 30 cells (grey area). Simulations reveal that the area marked with diagonal lines is where the entrainment is 1:3. The range of G_g values which allows 1:1 synchronization for a large number of cells is from about 0.25 to 0.4 nS.

These results demonstrate that small concentrations of IP_3, which do not elicit spontaneous calcium oscillations, support synchronization of activity in networks of cells. For this reason we used in this study an IP_3 concentration of 0.1 μM for the follower cells to further investigate the interaction between IP_3-mediated Ca-oscillations and action potentials. Summarizing, to completely synchronize a pacemaker and a single follower cell, a gap-junctional conductance near 0.06 nS is sufficient (Fig. 4), whereas for an infinitely long strand of cells the conductance must be in the range between 0.25 and 0.45 nS (Fig. 4). An explanation will be given below.

The current from the pacemaker cell through the gap junctions to the follower cells is given by $I_{gap}^{ij} = G_g(V_m^i - V_m^j)$ (Eq. 2). Increasing the electrical coupling (G_g) increases the leak of current from the pacemaker cell to its neighbor cells. If the net current to a follower cell is large enough and fast enough, the membrane potential might approach the threshold value near −40 mV for L-type Ca-channels. If that happens, the L-type Ca-channels open, causing an action potential and an inward current of Ca-ions. The increase of calcium in the cytosol activates the IP_3 receptor, leading to a calcium transient.

An opposite effect of increasing the electrical coupling is that it decreases the equivalent impedance of the network. Since the equivalent impedance Z_∞ for an infinitely large strand of follower cells decreases for increasing values of G_g ($\frac{\partial Z_\infty}{\partial R_g} > 0$ for all R_g; see Eq. 5), decreasing R_g (increasing G_g) implies a smaller value for Z_∞. If the equivalent impedance of the network decreases, the available current from the pacemaker cell spreads to a larger number of follower cells in the network, which makes it harder for the pacemaker cell to depolarise its neighboring follower cell to the threshold of the L-type Ca-channels for generation of an AP. In other words, a larger gap-junction conductance leads to a decrease in the effective impedance and to a smaller net current from the pacemaker cell to its neighboring follower cell, which explains the shift from 1:1 to 1:2 entrainment for strong coupling (G_g > 0.45 nS) in Fig. 4 and to 1:4 entrainment for G_g > 1.0 nS for network sizes in the range of 20 cells and more.

In conclusion, small coupling conductances prohibit a sufficiently large current from the pacemaker to the follower cell to reach the membrane threshold for excitation. For a large conductance the threshold for action potential generation cannot be reached since a large part of the current from the pacemaker to its neighboring follower cell flows to other follower cells, limiting the net current from pacemaker to its neighbor follower cell.

Entrainment of and propagation in a strand of electrically well coupled NRK cells

Failing AP transmission during strand entrainment

Fig. 5 shows the results of a simulation of the membrane potential behavior of a pacemaker cell in isolation (panel A, thick solid line) and that of a pacemaker cell (panel B, thick solid line) coupled to 100 follower cells (thin solid lines) in a strand with a gap-junctional conductance (G_g) of 3 nS. Note that this value for G_g is much larger than the values of G_g in

Figure 4. For G_g = 3 ns, the entrainment for a network of 20 cells or less is 1:1 and is 1:4 when the number of cells exceeds 30.

IP_3 concentrations are set to 1.0 μM and 0.1 μM for the pacemaker and follower cells, respectively. As shown in Fig. 4 this situation corresponds to 1:1 for a small number of follower cells (n < 17) and corresponds to 1:4 entrainment for n>20. This means that one out of every four calcium transients and APs generated by the pacemaker cell results into AP and calcium transients in the strand of follower cells. Fig. 5B shows an example where propagation does not take place. Fig. 6 shows a case where propagation does occur.

In Fig. 5A the uncoupled pacemaker cell (thick solid line) has an AP with a peak voltage near +10 mV, followed by a plateau phase near -20 mV. The AP is triggered by Ca^{2+} release from the ER store through the IP_3-receptor (E). The increased cytoplasmic Ca-concentration (C) causes depolarization of the cell by activation of the Ca-dependent Cl-channels. This depolarization to the Nernst potential of the Ca-dependent Cl-channels near -20 mV activates the L-type Ca-channel (G, I), which leads to a further increase in $\left[Ca_{cyt}^{2+}\right]$ (C).

The panels in the right hand column of Fig. 5 show the results when the pacemaker is coupled to 100 follower cells. Comparing the panels in the left and right column reveals some important differences between the results for an uncoupled pacemaker cell and for a pacemaker cell coupled to a strand of follower cells. The main difference relates to the slow and small increase of cytosolic calcium concentration in the pacemaker cell (panels C versus D, thick solid line) and the corresponding slow and small depolarization of the membrane potential (compare panels A and B) in the coupled situation for the pacemaker cell. Coupling the pacemaker cell to its neighboring follower cells by gap junctions causes the current from the pacemaker cell to leak away to the follower cells. As a result, depolarisation of the membrane potential of the pacemaker cell by the Ca-dependent Cl-channels reaches a lower peak value (panel B) and the level of activation of the L-type Ca-channels of the pacemaker

cell is not as high as in the case of the isolated pacemaker cell. This becomes clear by comparing the data in panels I and J, which show the activation gate (m, thick dashed-dotted line) and inactivation gate (h, thick solid line) for the uncoupled and coupled situation, respectively. For the uncoupled pacemaker cell the m gates open (panel I), which does not happen for the coupled pacemaker cell (panel J) leading to AP failure in the strand. As a consequence of the small activation of the L-type Ca-channels in the coupled pacemaker cell there is hardly any calcium inflow through the L-type Ca-channels into the cytosol (compare panel G with panel H and notice the different scales of the vertical axes). This also affects the boosting CICR by activation of the IP_3-receptor, because the smaller inflow of calcium through the L-type Ca-channel weakens CICR and results into a slower and smaller calcium flow through the IP_3-receptor (compare panels E and F) for the coupled pacemaker.

For the isolated pacemaker cell the fraction of open activation gates (f, thick dashed dotted line) increases rapidly followed by a slow closure of the inactivation gates (w, thick solid line in panel K). When the pacemaker is coupled to a strand of 100 follower cells the fraction of open activation gates does not reach as high values as for the isolated pacemaker (compare thick dashed -dotted lines in panels K and L). Notice that the fraction of open inactivation gates (w) is near 0.4 for the follower cells (thin solid lines in panel L, which all superimpose). The gate is not yet completely de-inactivated after the previous action potential, which has implications for the propagation of the AP as we will show when we compare Figs. 5 and 6.

In summary, when the pacemaker cell is coupled to a linear strand of follower cells, the membrane potential of the pacemaker cell increases much more slowly than in the uncoupled case, and does not reach as high values during the plateau phase due to the decreased flux of Ca-ions through the L-type Ca-channels and IP_3-receptor of the pacemaker cell. The depolarisation of the follower cells due to electrical coupling activates the L-type

Ca-channels in the follower cells only to a very small extent (panel J) and causes only a very small inflow of Ca-ions (panel H). This inflow is too small to induce a significant Ca^{2+}-induced Ca^{2+} release through the IP_3-receptor in the follower cells (thin solid line in panel F), because w is not yet sufficiently de-inactivated. As a consequence, a single pacemaker cell is not powerful enough to supply 1:1 entrainment between AP propagation and CaOs in a strand of NRK cells with $[IP_3] = 0.1\ \mu M$.

Entrained AP transmission

Fig. 6 shows the propagation of activity for a pacemaker cell coupled to 100 follower cells with a gap-junctional conductance (G_g) of 3 nS when the pacemaker cell succeeds in triggering AP propagation in the follower cells. In Fig. 6A the coupled pacemaker cell (thick solid line) depolarizes to -20 mV. This depolarization is triggered by Ca^{2+} release from the store through the IP_3-receptor (C). The increased cytoplasmic Ca-concentration causes depolarization of the cell by activation of the Ca-dependent Cl-channels. Note that the rise of the membrane potential for the pacemaker cell and its neighboring follower cells is much slower than that for distant follower cells. This causes a gradual start of the inactivation of the L-type Ca channel (decreasing h , solid lines in Fig. 6E) before activation m increases (dashed-dotted lines in 6E). Since the activation m in the pacemaker cell hardly increases above the value zero (thick dashed-dotted line in 6E), the L-type Ca-channels in the pacemaker cell hardly open (6D). For more distant follower cells, the rise of the membrane potential is much faster and activation m of the L-type Ca-channel increases rapidly, resulting in an action potential.

The depolarization of the pacemaker cell to the Nernst potential of the Ca-dependent Cl-channels near -20 mV activates the L-type Ca-channels in the neighboring follower cell slightly (hardly visible in D, see arrow), causing a small inflow of Ca-ions. Although the

inflow of calcium in the follower cells is small and hardly visible in Fig. 6D, the fraction of open inactivation gates (w) of the IP_3-receptor (solid lines panel F) is large enough to allow a significant Ca^{2+}-induced Ca^{2+} release (CICR) through the IP_3-receptor (see arrow, Fig. 6C). Moreover, the cytosolic Ca-concentration (B) due to small influx through the L-type Ca-channel (D) and through the IP_3-receptor (C) is large enough to cause full depolarisation to the Nernst potential of the Ca-dependent Cl-channels (A). The CICR through the IP_3-receptor in each follower cell reinforces the speed of their depolarization and, therefore, contributes to a better and stronger AP propagation in the one-dimensional array of cells.

The fraction of open activation (f, thick dashed-dotted lines) and inactivation (w) gates of the IP_3-receptor for a pacemaker cell (w, thick solid line) coupled to 100 follower cells (w, thin solid lines) are shown in panel F. Notice that the fraction of open w gates for the neighboring follower cells is a little higher than in Fig. 5K (thin solid lines). This is due to the small IP_3 concentration of 0.1 μM (see Eq. A.23), which gives a long time constant τ_w for de-inactivation. It takes about 300 seconds to re-open the inactivation gate w of the follower cells completely. Since the pacemaker cell generates an AP every 90 seconds, the inactivation gate (w) of the follower cells after a calcium transient has not recovered sufficiently at the next action potential of the pacemaker cell. This is clear in Fig. 5F, where the inactivation gates of the neighboring follower cell was 0.4, whereas it reaches values near 0.5 and 0.6 (thin solid lines) in Fig. 6F.

The main difference between Fig. 5 and Fig. 6 is that the inactivation gate w (thin solid lines) of the IP_3-receptor in the follower cells has recovered to higher values in Fig. 6F than in Fig. 5K. Therefore, the relatively small inflow of Ca-ions through the L-type Ca-channels is large enough to activate the IP_3-receptor by CICR in the first follower cell (see arrow, Fig. 6 panel C). The same occurs in the other follower cells. The membrane potential exerts a positive feedback on the Ca^{2+}-oscillator through Ca^{2+} influx through L-type Ca-

channels. On the other hand, the release of calcium through the IP_3-receptor exerts a positive feedback on the depolarization of the membrane. As a result, AP propagation with underlying CaOs is generated in the follower cells. This positive interaction between membrane excitability and IP_3 receptor explains why a small amount of IP_3 in the cell supports synchronization and propagation of activity in a network of cells.

We can understand the 1:4 entrainment of AP propagation (Figs. 5 and 6) by having a closer look at the de-inactivation time constant τ_w for the w gate. The time constant τ_w (Eq. A.23) determines the time for de-inactivation (w) of the IP_3-receptor, which depends among other things on $[IP_3]$. For low $[IP_3]$ values (near 0.1 μM) in the follower cells, the time constant τ_w of the inactivation gate w of the IP_3-receptor is long (in the order of 300 seconds). For high $[IP_3]$ near 1.0 μM in the pacemaker cell, τ_w is shorter and about 90 seconds. Since the time constant τ_w in the follower cells is long (about 300 s) relative to the time interval between APs generated by the pacemaker cell (about 90 s), the de-inactivation of the IP_3-receptor in the follower cells has not yet recovered after an action potential and IP_3-mediated calcium oscillation when the pacemaker cell generates the next action potential. This explains why 1:1 synchronization between pacemakers and followers is not possible in this case and why synchronization becomes harder for smaller amounts of IP_3 in the cell.

Propagation in a strand of cells

We will now address the experimental observation that action potentials and CaOs are propagated with a gap-junctional conductance G_g which is much larger (3 nS) than the predicted optimal gap-junctional coupling range for synchronization of a pacemaker to followers (range 0.25-0.4 nS in Fig. 4). We have to keep the following in mind: if the gap junction conductance is very small, the current from the pacemaker to the follower cell is too small to depolarize its neighbor cell rapidly and to sufficiently high membrane potential. If the

gap junction conductance is very large, the pacemaker cell is not able to provide enough current for depolarization of its neighboring cell, since most of the current flows through the network to other cells. As we will show, robust AP propagation and excitation of follower cells in the latter case can be achieved in the model in two ways: by increasing the conductance of the L-type Ca-channels and by increasing the number of pacemaker cells.

The first solution is to increase the conductance G_{CaL} of the L-type Ca-channel, which is helpful for both the pacemaker and the follower cells. With increased values of G_{CaL}, depolarization of the membrane potential of the pacemaker cell leads to a larger current through the L-type Ca-channels and to more current through the gap junctions. This generates a larger current from pacemaker to follower cells and makes it easier to reach the threshold level for opening of L-type Ca-channels in the follower cells. For follower cells a larger opening of their L-type Ca-channels leads to better facilitation of CICR through the IP_3-receptor. However, since it is known that the maximal value for G_{CaL} is close 1.6 nS (15), it would not be realistic to set G_{CaL} to higher values than the value of 1.6 nS, used in this study.

The second solution is to increase the number of terminal pacemaker cells in the one-dimensional network, which contributes to a larger current to the follower cells. When enough pacemakers are placed in the network, 1:1 AP propagation is observed. This is illustrated in Fig. 7, which shows the result of a simulation of a coupled strand with three terminal pacemakers (IP_3 = 1.0 μM) and 100 follower cells (IP_3 = 0.1 μM). The release of calcium from the ER to cytosol by the IP_3-receptor in the pacemaker cells (Fig. 7C) activates the Ca-dependent Cl-channels causing a depolarization to -20 mV (Fig. 7A). This depolarisation activates the L-type Ca-channels (Fig. 7D). Note the delay of the fluxes through the Ltype Ca-channels (panel D) relative to the fluxes through the IP_3-receptor (panel C). The depolarization of the three pacemaker cells causes a depolarization of the follower cells (panel

A) and action potentials by activation of their L-type Ca-channels of the followers (panel D). The three pacemakers cause 1:1 entrainment for the full network with 100 followers.

Differences in pacemaker and follower cells

Comparison of the behavior of the pacemaker cells and the follower cells in Fig. 7 shows some important differences. The first difference to be mentioned is the smaller peak of the AP in the pacemaker cells than in the follower cells (see Fig. 7A, compare thick solid lines with thin solid lines). In a pacemaker cell APs are triggered by IP_3-mediated intracellular CaOs. Each calcium transient leads to opening of the Ca-dependent Cl-channels causing a depolarisation of the pacemaker cell to the Cl-Nernst potential near -20 mV. This depolarisation opens the L-type calcium channels, which have a reversal potential near 50 mV. Since the calcium filling of the cytosol by release of calcium from the stores (see Fig. 7C) and the corresponding depolarisation to –20 mV due to activation of the chloride channels is slow (see Fig. 7A) relative to the activation and inactivation time constants of the L-type calcium channel, inactivation of the calcium L-type channels starts during the depolarisation to –20 mV. This explains why the inflow of calcium through the L-type calcium channel (Fig. 7D) and the initial peak of the action potential are smaller in pacemaker cells than in follower cells. The inward calcium flow through the L-type Ca-channels (Fig. 7D) is approximately twice as small for pacemaker cells than for follower cells.

Fig. 7 illustrates that three pacemaker cells are able to initiate propagating activity in a linear strand of follower cells, in which each has a small concentration of IP_3 ($[IP_3] = 0.1\ \mu M$) that assists in AP propagation through the network.

In Fig. 4 we showed that a single pacemaker could not induce propagating activity in a linear strand with a large number of follower cells for large gap-junctional conductance. With

three pacemakers 1:1 entrainment is obtained for gap-junctional conductances G_g above 0.25 nS.

Minimal value for G_{CaL}

As explained above, L-type Ca-channels are necessary for propagation of activity in a network of NRK fibroblasts (7). Fig. 8 shows the simulation results where we tried to find the minimum number of pacemaker cells as a function of G_{CaL} at a constant gap junction conductance of 3 nS. The minimal number of pacemaker cells required for stable 1:1 propagation of APs in a linear array of follower cells decreases for increasing G_{CaL}. The data points of the simulations in Fig. 8 reveal that no AP propagation is possible for G_{CaL} below 1.45 nS. Therefore in our model a critical minimal value for G_{CaL} is necessary for AP propagation in a network.

Discussion

The aim of this model study was to investigate how electrical coupling of excitable cells with IP_3-mediated calcium oscillations affects the initiation and propagation of Ca-waves in a strand of cells. IP_3-mediated calcium oscillations in two neighboring cells were coupled to the excitable membrane by cytosolic calcium as in Imtiaz et al. (22). Our general conclusion is that the interaction between IP_3-mediated calcium oscillations and action potentials in electrical coupled NRK cells provides a mechanism for fast calcium wave propagation and synchronization, in which the CICR component plays a significant supportive role.

The role of electrical coupling strength

The main result of this study is that it emphasizes the important functional role of the coupling between the excitable membrane and CICR from intracellular stores for calcium action potentials and the important role of electrical coupling between cells for the initiation and propagation of calcium action potentials. These results provide a better understanding of empirical results by Yao and Parker (48), who concluded that "electrical transmission may provide a means to 'leapfrog' slow chemical wave transmission and rapidly synchronize Ca^{2+} release within large individual cells and across populations of electrically coupled cells." A similar idea was reached by Sanders et al. (37), who based on a large set of empirical data concluded that "voltage-dependent Ca^{2+} entry that increases Ca^{2+} activity in pacemaker units near IP_3 receptors may be responsible for coordination of Ca^{2+} release events and entrainment of unitary currents within a network of ICC".

Fig. 3 shows entrainment for two heterogeneous pacemaker cells, which display full synchronization of intracellular CaOs for a coupling conductance (G_g) above 60 pS which is well in agreement with Imtiaz et al. (22) who found that weak electrical coupling is sufficient to synchronize heterogeneous cells of cell pairs. This result explains that at the physiological

gap-junctional coupling strength (3 nS) of NRK cells (Harks et al. (14)), the intracellular CaOs and APs of two oscillating cells are completely synchronized in phase. In the modelling study by Imtiaz et al. (22) it was reported that anti-phase behavior could occur for two weakly coupled cells for high oscillation frequencies, which is a well known result for interacting oscillators (9). This anti-phase coupling in their study is the result of the time constants involved in voltage-dependent IP_3 synthesis. Since it takes some time before changes in the membrane potential affect the production of IP_3, the effective coupling between cells by voltage-dependent IP_3-production has a frequency-dependent delay. Therefore, we conclude that voltage-dependent IP_3 synthesis cannot play an important role as it would disable synchronisation between cells to form a pacemaker cluster.

For low-frequency intracellular calcium oscillations, (typically one cycle per minute or lower) this delay is small relative to the period of the calcium oscillations, which results in in-phase behavior. For high-frequency intracellular calcium oscillations (2 cycles per minute or higher) the period of calcium oscillations is small relative to the time constant for production of IP_3, resulting in out-of-phase oscillations. In NRK cells, the highest oscillation frequencies are near one cycle per minute, but in general the oscillation frequency is much lower. Therefore, out-of-phase synchronization due to voltage-dependent IP_3 production does not happen in NRK cells and therefore, we did not include voltage-dependent IP_3-production.

Fig. 4 shows that synchronization of follower cells by a pacemaker cell is easier if the follower cells have a non-zero concentration of IP_3, allowing calcium transients by CICR. The CICR through the IP_3-receptor in each follower cell reinforces the speed of their depolarisation and, therefore, contributes to a better and stronger AP propagation in the one-dimensional array of cells. Moreover, Fig. 4 shows that entrainment and synchronization is optimal for a coupling between 0.25 and 0.45 nS, whereby 1:1 propagation of APs in the network is facilitated. However, the actual conductance of gap junctions between NRK cells

is approximately 3 nS, which is much larger than the optimal coupling range that follows from Fig. 4. In our view the relatively high conductance of 3 nS has at least two consequences.

The first one is that it prevents initiation of activity by a single pacemaker, but allows synchronized activity of a small cluster of pacemaker cells. It prevents spontaneous random activity by a single pacemaker cell and ensures robust initiation by a small cluster. For a linear strand at least three pacemakers are sufficient for propagation. Pilot studies for a two-dimensional network show that roughly 300 pacemaker cells are necessary to initiate propagating activity.

The second aspect related to the gap-junctional conductance relates to the velocity of propagation. A larger gap-junctional conductance gives a larger propagation velocity (36). Previous studies on propagation of activity in a network of non-excitable cells with IP_3-mediated calcium oscillations (10, 19, 20, 40) have shown that propagation may occur via diffusion of calcium and/or IP_3 through the gap junctions. Since diffusion is relatively slow relative to electrical coupling, the propagation velocity in such a network is typically in the range from 5-50 μm/s (19, 35, 38), which is much slower than propagation in excitable cells (typically 0.5 - 100 cm/s) and in our NRK cells (6, 16) where the propagation velocity is approximately a few mm/s.

The required number of pacemaker cells for exciting the strand

The analysis of the one-dimensional network in Figs. 5 and 6 with physiological electrical coupling (G_g = 3 nS), reveals that one terminal pacemaker cell cannot deliver sufficient current to the follower cells to obtain 1:1 synchronization and AP propagation in the cell strand. Increasing the value of the L-type calcium conductance alone would not help (see Fig. 8). The minimal number of pacemaker cells required to initiate AP propagation depends on

the [IP_3] of the follower cells (compare results for [IP_3] = 0 and [IP_3] = 0.1 in follower cells in Fig. 4), and critically depends on the conductance of the L-type Ca-channels (G_{CaL}), which needs to be larger than 1.45 nS to facilitate propagation of APs at all (Fig. 8). In this study we have fixed G_{CaL} at 1.6 nS, which results into a requirement of 3 pacemaker cells for 1:1 propagation of APs in the one-dimensional network.

Chemical coupling versus electrical coupling

We have shown that calcium waves and propagation of action potentials can be achieved by a mechanism where depolarization by action potential firing and calcium triggered opening of chloride channels causes an action potential and intracellular calcium transient in its neighbor cell. Such a coupling mechanism is significantly more effective than that of the chemical coupling based class of models, as a membrane potential change has a quick coupling effect over distances several orders of magnitude greater than either diffusion of Ca^{2+} or IP_3 through gap junctions (40).

Both Ca^{2+} and IP_3 have been shown to permeate through gap junctions by diffusion. This mechanism plays a crucial role in the propagation of Ca-waves in networks with nonexcitable cells (10, 19, 20, 40). In our study with excitable cells, the electrical coupling and the relatively fast dynamics of the L-type Ca-channel provide a much faster propagation than in non-excitable cells. Since diffusion of Ca^{2+} and IP_3 takes place on a time scale, much longer than the time scale of propagation by electrical coupling and activation of the L-type Ca-channels, we have not incorporated diffusion of Ca^{2+} and IP_3 in our study.

In a recent study Tsaneva-Atanasova et al. (43) have suggested that intercellular calcium diffusion is necessary and sufficient to synchronize the oscillations in neighboring cells with different intrinsic oscillation frequencies. The results of our study indicate that intercellular calcium diffusion may be sufficient but is not necessary, since coupling of

intracellular CaOs by the excitable membrane and electrical intercellular coupling also achieves synchronization of pacemaker cells with different intrinsic oscillation frequencies.

Several studies (see e.g. Höfer et al. (19)) calculated the minimal gap-junctional permeability for calcium, which is required for calcium wave propagation, as a function of the diffusion coefficient for calcium. The minimal value is found to be about 0.05 μm sec^{-1}, which gives an inflow of about 0.25 $\times 10^{-6}$ μmol in our cell. The result of our model study show that the total change of calcium concentration in the cytosol due to inflow through the L-type Ca-channels is about 100 $\times 10^{-6}$ μmol per action potential this is much larger than the change due to diffusion of calcium, which explain why the propagation of Ca-waves mediated by the L-type Ca-channels is faster and more robust.

In the present model study agonist or IP_3 diffusion may improve local synchronization of the surrounding follower cells by smoothing the sensitivities of the CICR mechanism.

Voltage-dependent gap-junctional conductance

In our study the gap-junctional conductance is assumed to be independent on the voltage of the membrane. However, it is well known that the gap-junctional conductance is not constant but voltage dependent. The gap-junctional conductance between two cells may decrease up to 20 % during an action potential compared to the steady-state conductance without any voltage difference across the gap junction. In a recent study using transfected neuroblastoma cells, inactivation kinetics of connexin43 were studied by imposing an AP clamp instead of a rectangular voltage pulse on one of the cells (30). These experiments showed that, following the peak of the AP, the junctional conductance decreased within 25 ms to 58 % of control. These relatively slow time constants are in agreement with experimental observations (2),which indicate that the transition rates for the gap junction channels are significantly longer than the time constant of the cell membrane, which is about 1 ms. Comparison of these

inactivation times to transjunctional conduction times observed during steady state propagation under conditions of severe uncoupling suggests that gap junctional gating has only a minor effect on overall conduction velocities (36).

Functional implications

The results of this study show that the coupling of intracellular calcium oscillations and action potential firing causes propagation of activity through a network of cells, which is robust and much faster than propagation of calcium waves in a network of non-excitable cells (12, 19, 20, 43).

Calcium-induced calcium release through the IP_3-receptor, triggered by calcium inflow through L-type Ca-channels during an action potential supports cell depolarization by activation of Ca-dependent Cl-channels. This boosting of propagation of activity by CICR provides a robust mechanism, which is also found in gastrointestinal cells (44), urethral cells (4, 22) and in heart pacemaker cells (31). In all these cell types robust pacemaking and propagation of activity is crucially important for the function of the cell network in the organism.

In smooth muscle cells oscillatory release of Ca^{2+} through IP_3 receptors and voltage-dependent Ca^{2+} influx through L-type Ca-channels underlie rhythmic vasomotion (1, 50). Spontaneous calcium waves occurring after a long action potential plateau may also modulate the removal of voltage dependent inactivation of L-type Ca^{2+} channels, and affect the likelihood of the occurrence of early afterdepolarizations (48). Spontaneous CaOs may be implicated in diverse manifestations of heart failure–impaired systolic performance, increased diastolic tonus, and an increased probability for the occurrence of arrhythmias (48). Therefore, the outcomes of this model study are also of interest for understanding mechanisms of pacemaker synchronization and AP propagation in many other systems.

Conclusion

Consistent with experimental observations for NRK cells (30), we showed that electrical intercellular coupling is sufficient for synchronizing CaOs of pacemaker cells and for propagation of AP coupled calcium waves over a linear network of cells. For NRK cells it has become clear that membrane excitation can evoke and enhance release of Ca^{2+} from the ER store via voltage-dependent Ca^{2+} inflow through L-type Ca-channels. Our general message is that some form of CICR interaction with or caused by Ca inflow through voltage dependent Ca-channels can boost propagation of electrical excitation and its continuous calcium oscillations. Any form of CICR, ryanodine-mediated receptors are another example, would engage a similar interaction.

Acknowledgments

This research project was funded by the Netherlands Organization for Scientific Research (NWO; project 805.47.066).

Appendix: Equations

This appendix gives an overview of the equations that are relevant for the dynamics of the membrane potential and intracellular calcium oscillation. For further details, see Kusters et al. (2005).

$$C_m \frac{dV_m}{dt} = -\left(I_{Kir} + I_{lk} + I_{CaL} + I_{Cl(Ca)} + I_{SDC}\right) \tag{A1}$$

$$I_{Kir} = G_{Kir}\sqrt{\frac{K_0}{K_{ost}}}\left(\frac{\alpha}{\alpha+\beta}\right)(V_m - E_K) \tag{A2}$$

$$\alpha = \frac{0.1}{1+\exp\{0.06(V_m - E_K - 50)\}} \tag{A3}$$

$$\beta = \frac{3\times\exp\{0.0002(V_m - E_K + 100)\} + \exp\{0.0002(V_m - E_K - 10)\}}{1+\exp\{-0.06(V_m - E_K - 50)\}} \tag{A4}$$

$$E_K = 1000\frac{RT}{F}\ln\left(\frac{K_0}{K_i}\right) \tag{A5}$$

$$I_{lk} = G_{lk}\left(V_m - E_{lk}\right) \tag{A6}$$

$$I_{CaL} = mhG_{CaL}(V_m - E_{CaL}) \tag{A7}$$

$$m_\infty = \frac{1}{1+\exp\left(-\frac{V_m+10}{5.24}\right)} \tag{A8}$$

$$\tau_m = 0.005\frac{m_\infty\left(1-\exp\left(-(V_m+10)/5.9\right)\right)}{0.035(V_m+10)} \tag{A9}$$

$$h_\infty = \frac{1}{1+\exp\left(\frac{V_m+37}{4.6}\right)} \tag{A10}$$

$$\tau_h = \frac{0.02}{0.02+0.0197\exp\left\{-\left[0.0337(V_m+10)\right]^2\right\}} \tag{A11}$$

$$I_{Cl(Ca)} = \frac{\left[Ca^{2+}_{cyt}\right]}{\left[Ca^{2+}_{cyt}\right]+K_{Cl(Ca)}}G_{Cl(Ca)}\left(V_m - E_{Cl(Ca)}\right) \tag{A12}$$

$$I_{SDC} = \frac{K_{SDC}}{\left[Ca^{2+}_{cyt}\right] + K_{SDC}} G_{SDC}\left(V_m - E_{SDC}\right) \tag{A13}$$

$$\frac{d[BCa]}{dt} = k_{on}\left(\left[T_B\right] - [BCa]\right)\left[Ca^{2+}_{cyt}\right] - k_{off}[BCa] \tag{A14}$$

$$J_{PM} = -\frac{10^{-6}}{z_{Ca}F}\frac{1}{A_{PM}}\left(I_{CaL} + I_{SDC}\right) - J_{PMCA} \tag{A15}$$

$$J_{PMCA} = J^{\max}_{PMCA}\frac{\left[Ca^{2+}_{cyt}\right]}{\left[Ca^{2+}_{cyt}\right] + K_{PMCA}} \tag{A16}$$

The equations defining the properties of the IP_3-mediated intracellular calcium dynamics are the following

$$Vol_{cyt}\frac{d\left[Ca^{2+}_{cyt}\right]}{dt} = A_{ER}\left(J_{lkER} + J_{IP_3R} - J_{SERCA}\right) - \frac{d[BCa]}{dt}Vol_{cyt} + A_{PM}J_{PM} \tag{A17}$$

$$Vol_{ERt}\frac{d\left[Ca^{2+}_{ER}\right]}{dt} = A_{ER}\left(-J_{lkER} - J_{IP_3R} + J_{SERCA}\right) \tag{A18}$$

$$J_{lkER} = K_{lkER}\left(\left[Ca^{2+}_{ER}\right] - \left[Ca^{2+}_{cyt}\right]\right) \tag{A19}$$

$$J_{IP_3R} = f_\infty^3 w^3 K_{IP_3R}\left(\left[Ca^{2+}_{ER}\right] - \left[Ca^{2+}_{cyt}\right]\right) \tag{A20}$$

$$f_\infty = \frac{\left[Ca^{2+}_{cyt}\right]}{K_{fIP_3} + \left[Ca^{2+}_{cyt}\right]} \tag{A21}$$

$$w_\infty = \frac{\dfrac{\left[IP_3\right]}{K_{wIP_3} + \left[IP_3\right]}}{\dfrac{\left[IP_3\right]}{K_{wIP_3} + \left[IP_3\right]} + K_{w(ca)}\left[Ca^{2+}_{cyt}\right]} \tag{A22}$$

$$\tau_\infty = \frac{a}{\dfrac{\left[IP_3\right]}{K_{wIP_3} + \left[IP_3\right]} + K_{w(ca)}\left[Ca^{2+}_{cyt}\right]} \tag{A23}$$

$$J_{SERCAA} = J^{\max}_{SERCA}\frac{\left[Ca^{2+}_{cyt}\right]^2}{\left[Ca^{2+}_{cyt}\right]^2 + K^2_{SERCA}} \tag{A24}$$

References

[1] Aalkjaer, C., and H. Nilsson. 2005. Vasomotion: cellular background for the oscillator and for the synchronization of smooth muscle cells. *Br. J. Pharmacol.* 144:605–616.

[2] Baigent, S. 2003. Cells coupled by voltage-dependent gap junctions: the asymptotic dynamical limit. *Biosystems* 68(2-3):213–22.

[3] Bukauskas, F. F., A. Bukauskiene, and V. K. Verselis. 2002. Conductance and permeability of the residual state of connexin43 gap junction channels. *J. Gen. Physiol.* 119:171–185.

[4] Cousins, H. M., F. R. Edwards, H. Hickey, C. E. Hill, and G. D. Hirst. 2003. Electrical coupling between the myenteric interstitial cells of Cajal and adjacent muscle layers in the guinea-pig gastric antrum. *J. Physiol.* 550:829–44.

[5] Cuthbertson, K. S., and P. H. Cobbold. 1985. Phorbol ester and sperm activate mouse oocytes by inducing sustained oscillations in cell Ca^{2+}. *Nature* 316:541–542.

[6] de Roos, A. D., P. H. Willems, P. H. Peters, E. J. van Zoelen, and A. P. Theuvenet. 1997. Synchronized calcium spiking resulting from spontaneous calcium action potentials in monolayers of NRK fibroblasts. *Cell Calcium* 22:195–207.

[7] de Roos, A. D., P. H. Willems, E. J. van Zoelen, and A. P. Theuvenet. 1997. Synchronized Ca^{2+} signaling mediated by intercellular propagation of Ca2+ action potentials in monolayers of NRK fibroblasts. *Am. J. Physiol.* 273:C1900–1907.

[8] Dupont, G., and A. Goldbeter. 1993. One-pool model for Ca^{2+} oscillations involving Ca^{2+} and inositol 1,4,5-trisphosphate as co-agonists for Ca^{2+} release. *Cell Calcium* 14:311–322.

[9] Ernst U., K. Pawelzik, and T. Geisel. 1998. Delay-induced multistable synchronization of biological oscillators. *Phys Rev E* 57 (2): 2150-2162.

[10] Falcke, M. 2004. Reading the patterns in living cells - the physics of Ca^{2+} signaling. *Adv. Phys.* 53:255–440.

[11] Fogarty, K., J. Kidd, D. Tuft, and P. Thorn. 2000. Mechanisms underlying insp3-evoked global Ca^{2+} signals in mouse Pancreatic Acinar cells. *J. Physiol* 526:515–526.

[12] Freiesleben de Blasio, B., J. Iversen, and J. A. Rottingen. 2004. Intercellular calcium signalling in cultured renal epithelia: a theoretical study of synchronization mode and pacemaker activity. *Eur. Biophys J* 33:657–670.

[13] Harks, E. G., A. D. De Roos, P. H. Peters, L. H. de Haan, A. Brouwer, D. L. Ypey, E. J. van Zoelen, and A. Theuvenet. 2001. Fenamates: a novel class of reversible gap junction blockers. *J. Pharmacol. Exp. Ther.* 298:1033–1041.

[14] Harks, E. G., J. J. Torres, L. N. Cornelisse, D. L. Ypey, and A. P. Theuvenet. 2003. Ionic basis for excitability in normal rat kidney (NRK) fibroblasts. *Am. J. Physiol. Cell Physiol.* 196:493–503.

[15] Harks, E. G., W. J. Scheenen, P. H. Peters, E. J. V. Zoelen, and A. P. Theuvenet. 2003. ProstaglandinF2-alpha induces unsynchronized intracellular calcium oscillations in monolayers of gap junctionally coupled NRK fibroblasts. *Pflügers Arch.* 447:78–86.

[16] Harks, E. G. 2003c. *Excitable Fibroblast! Ion channels, gap junctions, action potentials and calcium oscillations in Normal Rat Kidney Fibroblasts.* PhD-thesis, Radboud University Nijmegen.

[17] Henriquez, C. S., and R. Plonsey. 1987. Effect of resistive discontinuities on waveshape and velocity in a single cardiac fibre. *Med. Biol. Eng. Comput.* 25(4):428–38.

[18] Henriquez, A. P., R. Vogel, B. J. Muller-Borer, C. S. Henriquez, R. Weingart, and W. E. Cascio. 2001. Influence of dynamic gap junction resistance on impulse propagation in ventricular myocardium: A computer simulation study. *Biophys. J.* 81:2112–2121.

[19] Höfer, T., A. Politi, and R. Heinrich. 2001. Intercellular Ca^{2+} wave propagation through gap-junctional Ca^{2+} diffusion: A theoretical study. *Biophys. J* 80:75–87.

[20] Höfer, T., L. Venance, and C. Giaume. 2002. Control and plasticity of intercellular calcium waves in astrocytes: A modeling approach. *J. Neurosci* 22:4850–4859.

[21] Imtiaz, M. S., D. W. Smith, and D. F. van Helden. 2002. A theoretical model of slow wave regulation using voltage-dependent synthesis of inositol 1,4,5-trisphosphate. *Biophys. J.* 83:1877–1890.

[22] Imtiaz, M. S., C. P. Katniky, D. W. Smith, and D. F. van Helden. 2006. Role of Voltage-dependent modulation of store Ca^{2+} release in synchronization of Ca^{2+} oscillations. *Biophys. J.* 90:123.

[23] Joyner, R. W., J. Picone, R. Veenstra, and D. Rawling. 1983. Propagation through electrically coupled cells. Effects of regional changes in membrane properties. *Circ. Res* 53:526–534.

[24] Joyner, R. W., R. Veenstra, D. Rawling, and A. Chorro. 1984. Propagation through electrically coupled ells. Effects of a resistive barrier. *Biophys J.* 45:1017–1025.

[25] Joyner, R. W., and F. J. L. van Capelle. 1986. Propagation through electrically coupled cells. *Biophys J.* 50:1157–1164.

[26] Keener, J. P. 1991. The effects of discrete gap junction coupling on propagation in myocardium. *J. Theor. Biol.* 148:49–82.

[27] Kusters, J. M. A. M., M. M. Dernison, W. P. M. van Meerwijk, D. L. Ypey, A. P. R. Theuvenet, and C. C. A. M. Gielen. 2005. Stabilizing role of calcium store-dependent plasma membrane calcium channels in action-potential firing and intracellular calcium oscillations. *Biophys. J.* 89:3741–3756.

[28] Kusters, J. M. A. M., J. M. Cortes, W. P. M. van Meerwijk, D. L. Ypey, A. P. R. Theuvenet, and C. C. A. M. Gielen. 2007. Hysteresis and bi-stability in a realistic cell-model for calcium oscillations and action potential firing. *Phys. Rev. Lett.* 234:24.

[29] Lakatta, E., A. Talo, M. C. Capogrossi, H. Spurgeon, and M. D. Stern. 1992. Spontaneous sarcoplasmic reticulum Ca^{2+} release leads to heterogeneity of contractile and electrical properties of the heart. *Basic Res. Cardiol.* 87:93–104.

[30] Lin, L., M. Crye, and R. D. Veenstra. 2003. Regulation of connexin43 gap junctional conductance by ventricular action potentials. *Circ. Res.* 93:63–73.

[31] Maltsev, V., T. Vinogradova, and E. Lakatta. 2006. The emergence of a general theory of the initiation and strength of the heartbeat. *J. Pharmacol. Sci.* 100:338.

[32] Minneman, K. P. 1988. Alpha 1-adrenergic receptor subtypes, inositol phosphates, and sources of cell Ca^{2+}. *Pharmacol. Rev.* 40:87–119.

[33] Nathanson, M., P. P. A. O'Sullivan, A. Burgstahler, and J. Jamieson. 1992. Mechanism of Ca^{2+} wave propagation in pancreatic acinar cells. *J. Biol. Chem.* 267:18118–18121.

[34] Pikovsky, A., M. Rosenblum, and J. Kurths. 2003. *Synchronization: A universal concept in nonlinear sciences*. Cambridge University Press.

[35] Politi, A., L. D. Gaspers, A. P. Thomas, and T. Hofer. 2006. Models of IP_3 and Ca^{2+} oscillations: frequency encoding and identification of underlying feedbacks. *Biophys. J.* 90(9):3120–33.

[36] Rohr, S. 2004. Role of gap junctions in the propagation of the cardiac action potential. *Cardiovasc. Res.* 62:309–322.

[37]Sanders, K.M., S.D. Koh, and S.M. Ward. 2006 Interstitial cells of Cajal as pacemakers in the gastrointestinal tract. *Ann. Rev. Physiol.* 68: 307-343.

[38] Sanderson, M. J., A. C. Charles, S. Boitano, and E. R. Dirksen. 1994. Mechanisms and function of intercellular calcium signaling. *Mol. Cell. Endocrinol.* 98:173–187.

[39] Savineau, J. P., and R. Marthan. 2000. Cytosolic calcium oscillations in smooth muscle cells. *News Physiol. Sci.* 15:50–55.

[40] Sneyd, J., B. T. R. Wetton, A. C. Charles, and M. Sanderson. 1995. Intercellular calcium waves mediated by diffusion of inositol triphosphate: a 2-dimensional model. *Am. J. Physiol. Cell Physiol.* 37:C1537–C1545.

[41] Tong, D., J. E. I. Gittens, G. M. Kidder, and D. Bai. 2006. Patch-clamp study reveals that the importance of connexin43-mediated gap junctional communication for ovarian folliculogenesis is strain specific in the mouse. *Am. J. Physiol. Cell Physiol.* 290:C290–C297.

[42] Torres, J. J., L. N. Cornelisse, E. G. A. Harks, W. P. M. van Meerwijk, A. P. R. Theuvenet, and D. L. Ypey. 2004. Modeling action potential generation and propagation in NRK fibroblasts. *Am. J. Physiol. Cell Physiol.* 287:C851–C865.

[43] Tsaneva-Atanasova, K. T., D. Yule, and J. Sneyd. 2004. Calcium oscillations in a triplet of Pancreatic Acinar cells. *Biophys. J.* 88:1535–1551.

[44] Torihashi, S., T. Fujimoto, C. Trost, and S. Nakayama. 2002. Calcium oscillation linked to pacemaking of interstitial cells of cajal. *J. Biol. Chem.* 277(21):19191.

[45] Van Helden, D. F., and M. S. Imtiaz. 2003. Ca^{2+} phase waves: a basis for cellular pacemaking and long-range synchronicity in the guinea pig gastric pyloris. *J. Physiol.* 548:271–296.

[46] Verheijck, E. E., R. Wilders, R. W. Joyner, D. A. Golod, R. Kumar, H. J. Jongsma, L. N. Bouman, and A. C. van Ginneken. 1998. Pacemaker synchronization of electrically coupled rabbit sinoatrial node cells. *J. Gen. Physiol.* 111(1):95–112.

[47] Woods, N. M., K. S. Cuthbertson, and P. H. Cobbold. 1986. Repetitive transient rises in cytoplasmic free calcium in hormone-stimulated hepatocytes. *Nature* 319:600–602.

[48] Yao Y., and I. Parker. 1994. Ca^{2+} influx modulation of temporal and spatial patterns of inositol triphosphaste-mediated Ca^{2+} liberations in Xenopus-oocytes. *J. Physiol. (London)* 476 (1): 17-28.

[49] Ypey, D. L., W. P. M. VanMeerwijk, and R. L. DeHaan. 1982. *Synchronization of cardiac pacemaker cells by electrical coupling*. Nijhoff, The Hague.

[50] Zhao, J., M. Imtiaz, and D. van Helden. 2002. Ca^{2+} oscillations and pacemaker potentials underlying vasomotion in guinea-pig lymphatic smooth muscle. *Proc. Aust. Health Med. Res. Cong.* Abstr. 1148.

Figure Legends

Fig. 1.

A. The electrical circuit for a one-dimensional network, where a pacemaker cell (”P”) is coupled by a resistance R_g to n follower cells. Each follower cell is represented by a capacitance C and resistance R_f and is coupled to its neighbors by gap junctions with a resistance R_g. B. The expansion of a network with n follower cells with an extra follower cell. C. Schematic circuit of a pacemaker cell coupled to an infinitely large strand of cells with a total impedance Z_∞.

Fig. 2.

Phase response curves of a single cell to depolarizing current pulses of 10, 15 and 20 pA of 50 ms duration (A) and to calcium pulses associated with a calcium current injection of 1, 2 and 5 pA of 50 ms duration (B). The top three subpanels show an example of the effect of current (15 pA in panels A) and calcium pulses (1 pA in panels B) on the phase advance of the AP and CaO (dashed lines). Solid lines show the AP and CaO without perturbation. The lower panels of A and B show the phase change of the IP_3-mediated calcium oscillator as a function of the timing of the current pulse and calcium pulse, respectively. The lower left panel show the phase change as a function of phase to a current pulse of 10 pA (thick solid line), 15 pA (dashed-dotted line) and 20 pA (thin solid line). The lower right panel shows the phase change as a function of phase to a calcium pulse of 1 pA (thick solid line), 2 pA (dashed-dotted line) and 5 pA (thin solid line). The dashed lines are linear interpolations between PRC-values calculated at steps of 0.1.

Fig. 3.

The Arnold tongues for two heterogeneous coupled cells as a function of the gap junction coupling conductance G_g. The IP_3 concentration of one cell is set to a value of 1.0 μM, while the IP_3 concentration of the second cell is varied in steps of 0.005 μM at a rate of one step

per 9000 seconds from 0.0 μM to 8.0 μM. It shows only the regions for the major entrainment ratio's (1:2 (dotted pattern), 2:3 (oblique lines), 1:1 (white), 4:3 (squared pattern) and 3:2 (grey)).

Fig. 4.

The entrainment areas for a one-dimensional network with one terminal pacemaker cell (IP_3 concentration 1.0 μM) and follower cells (solid lines for IP_3 concentration 0.1 and dashed lines for 0.0 μM, respectively) as a function of number of cells (#) and gap junction coupling (G_g).

Fig. 5.

The membrane potential (panels A and B), cytosolic calcium concentration [$Ca2+_{cyt}$] (panels C and D), the calcium flow through the IP_3-receptor (panels E and F), the calcium flow through the L-type Ca-channels (panels G and H) and its fraction of open activation (m, thick dashed-dotted line) and inactivation (h, thick solid line) gates (panels I and J) for an isolated pacemaker cell (thick solid lines, left panels) and for a pacemaker cell (thick solid lines, right panels) coupled to 100 follower cells (thin solid lines). The fraction of open activation (f) and inactivation (w) gates of the IP_3-receptor for a pacemaker cell (f, thick dashed-dotted line and w, thick solid line in panels K and L) coupled to 100 follower cells (f, thin dashed-dotted line and w, thin solid line, with G_g = 3 nS) are shown in panel L. $\frac{d}{dt}\left[Ca^{2+}\right]_{IP_3}$ and $\frac{d}{dt}\left[Ca^{2+}\right]_{CaL}$ represent the change in calcium concentration due to calcium inflow through the IP_3-receptor and L-type Ca-channel, respectively.

Fig. 6.

The membrane potential (A), cytosolic calcium concentration $\left[Ca^{2+}_{cyt}\right]$ (B), the calcium flow through the IP_3-receptor (C), the calcium flow through the L-type Ca-channel (D) and the fraction of open activation (m, dashed lines) and inactivation (h, solid lines) gates (E) for a pacemaker cell (thick lines) coupled to (Gg = 3 nS) 100 follower cells (thin lines). The

fraction of open activation (f) and inactivation (w) gates of the IP_3-receptor for a pacemaker cell (f, thick dashed-dotted line and w, thick solid line) coupled to 100 follower cells (f, thin dashed-dotted lines and w, thin solid lines) are shown in F. Arrows indicate where a small inflow of calcium by the L-type calcium channel (Fig. D) causes a small CICR through the IP_3 receptor (C). Note the different scales for calcium flow for C and D.

Fig. 7.

The membrane potential (A), cytosolic calcium concentration $\left[Ca^{2+}_{cyt}\right]$ (B), the calcium flow through the IP_3-receptor channel (C) and the calcium flow through the L-type Ca-channel (D) for a one-dimensional network with three pacemaker cells (thick solid lines) coupled to 100 follower cells (thin solid lines). IP_3 concentrations are set to 1.0 μM and 0.1 μM for the pacemaker and follower cells, respectively.

Fig. 8.

The simulation results (open dots) for 1:1 synchronization and propagation of APs as a function of the conductance of the L-type Ca-channel (G_{CaL}) and number of pacemaker cells (#) for a constant gap junctional conductance of 3 nS. No propagation takes place for G_{CaL} < 1.4 nS whatever the number of pacemaker cells.

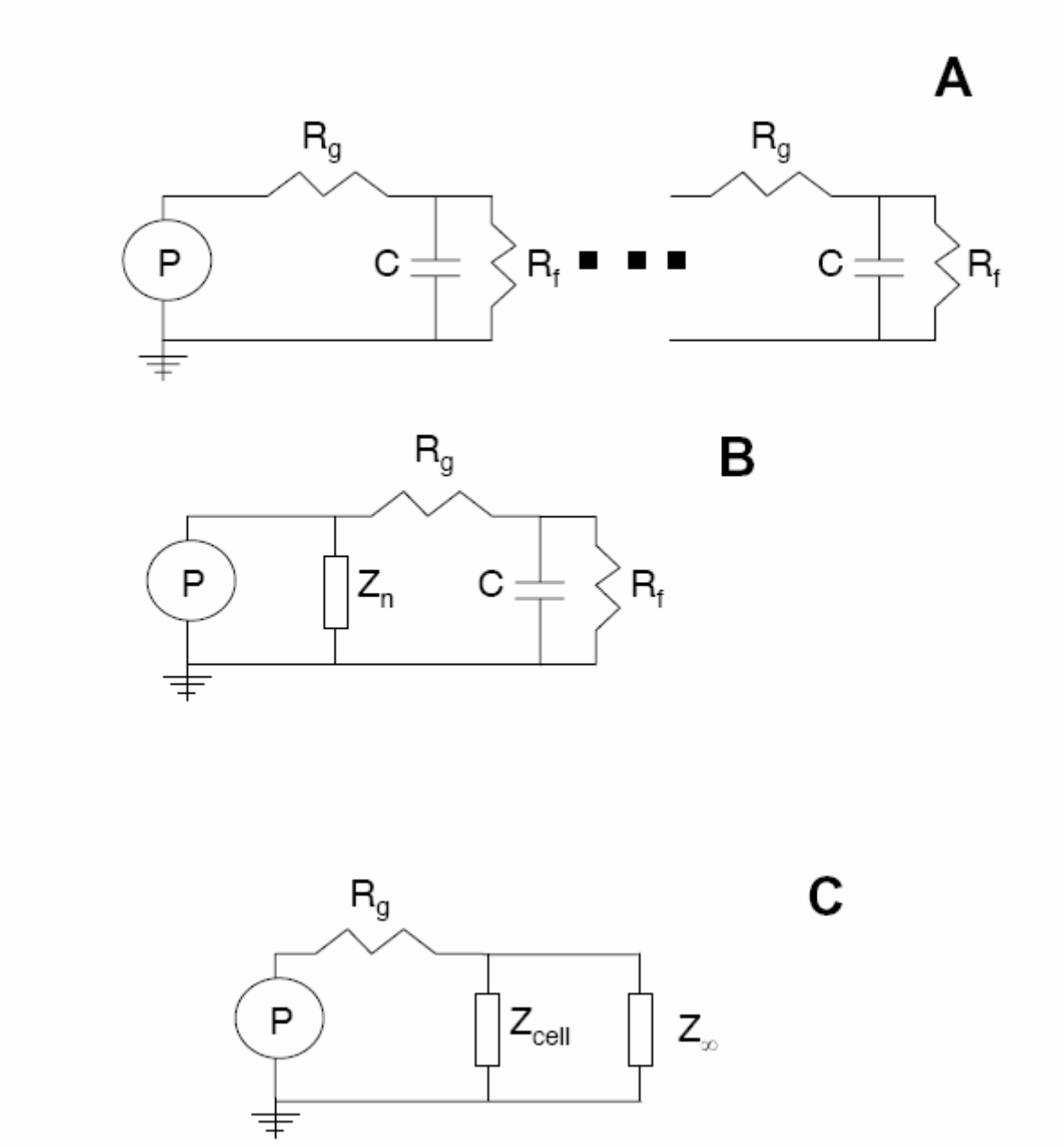

Figure 1

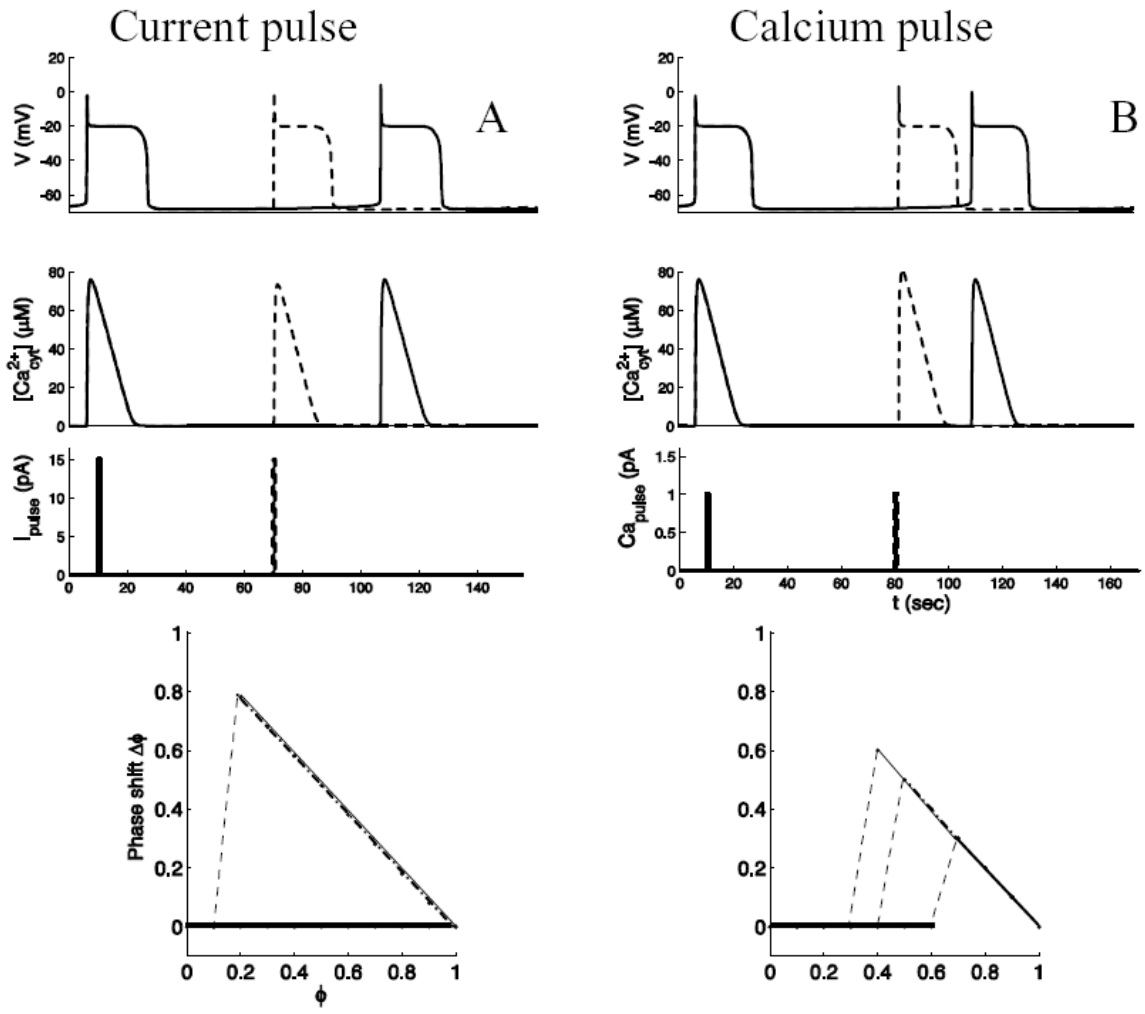
Current pulse
Calcium pulse
A
B
V (mV)
[Ca2+cyt] (μM)
Ipulse (pA)
Capulse (pA
t (sec)
Phase shift Δϕ
ϕ

Figure 2

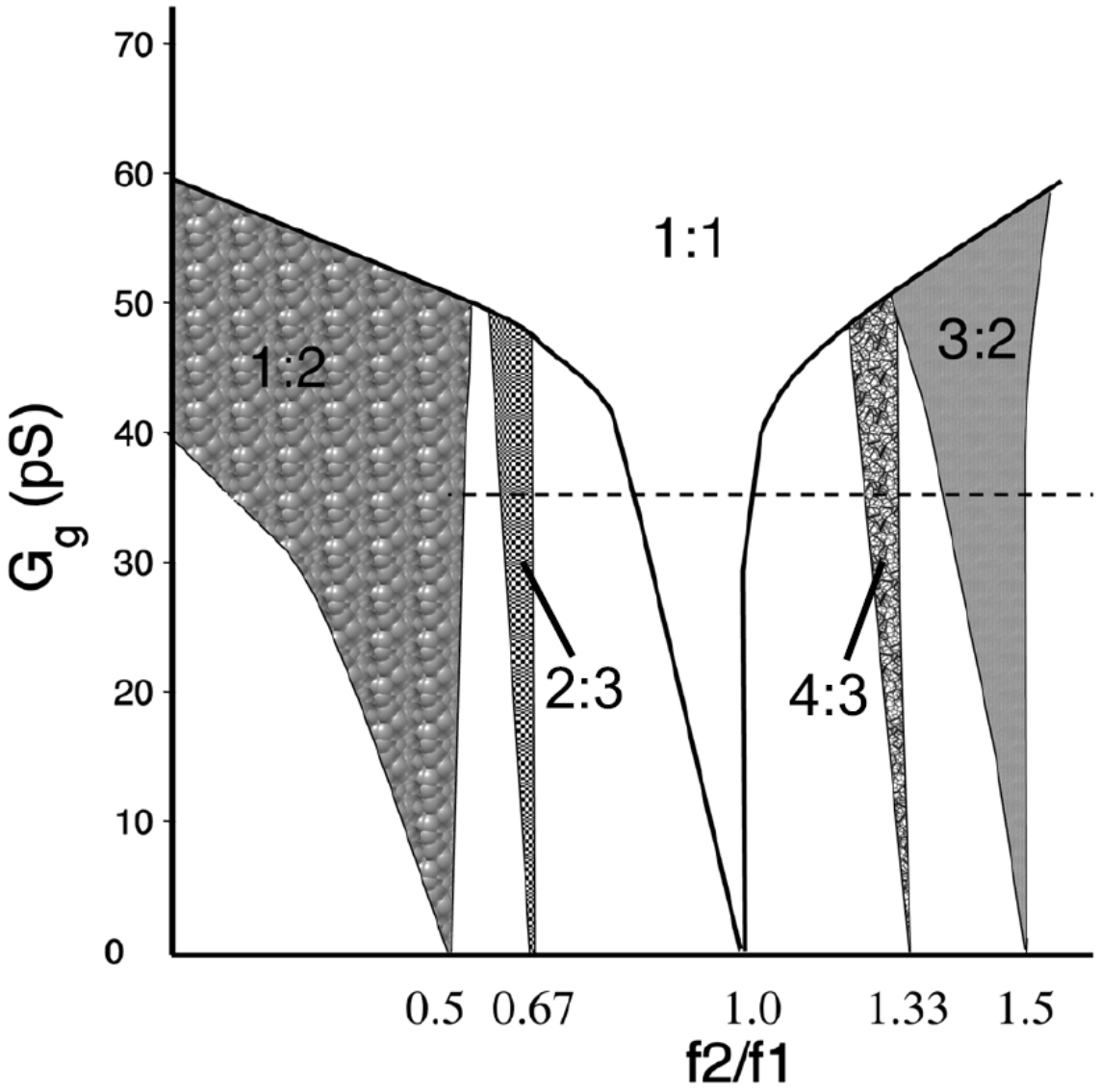

Figure 3

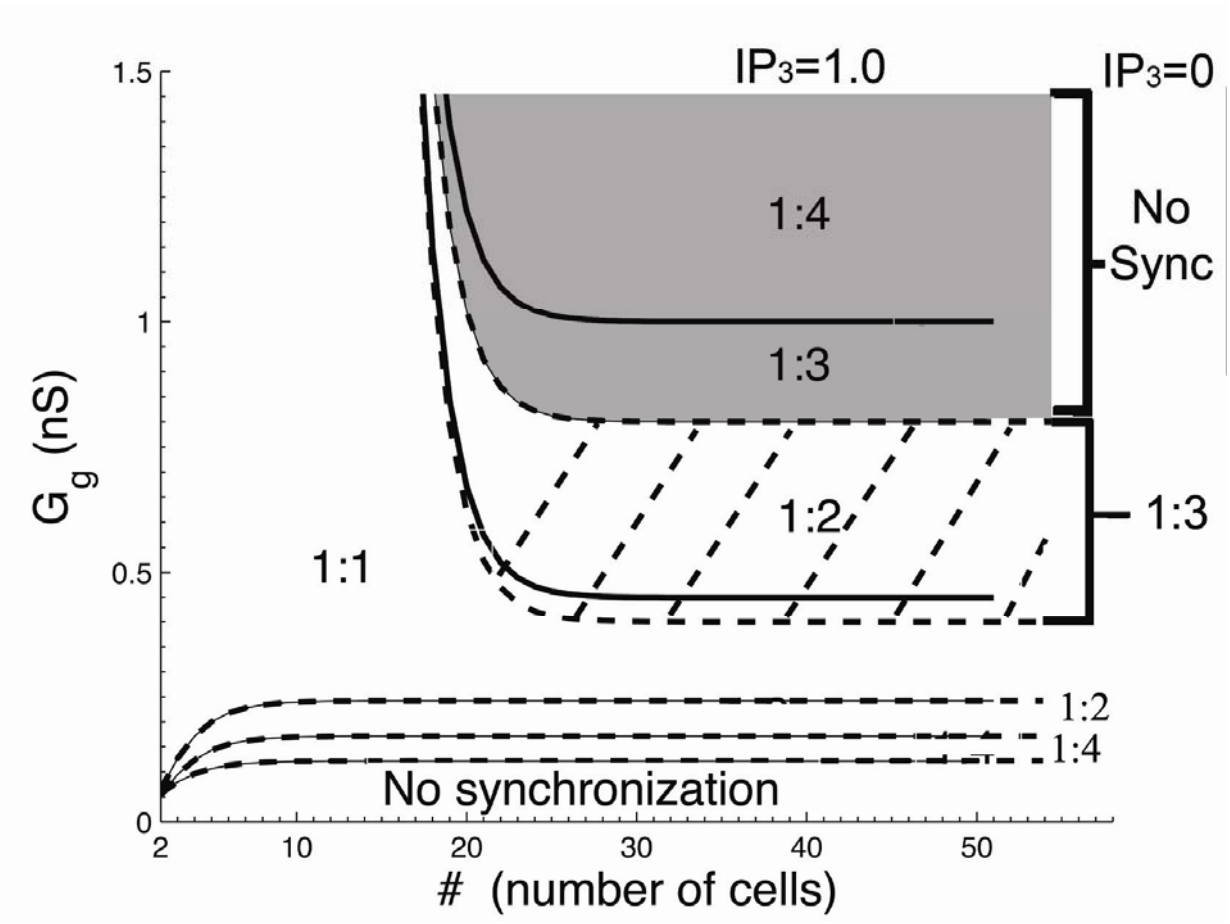
IP3=1.0
IP3=0
1:4
No
Sync
1:3
1:2
1:3
1:1
1:2
1:4
No synchronization
Gg (nS)
(number of cells)
1.5
1
0.5
0
2
10
20
30
40
50

Figure 4

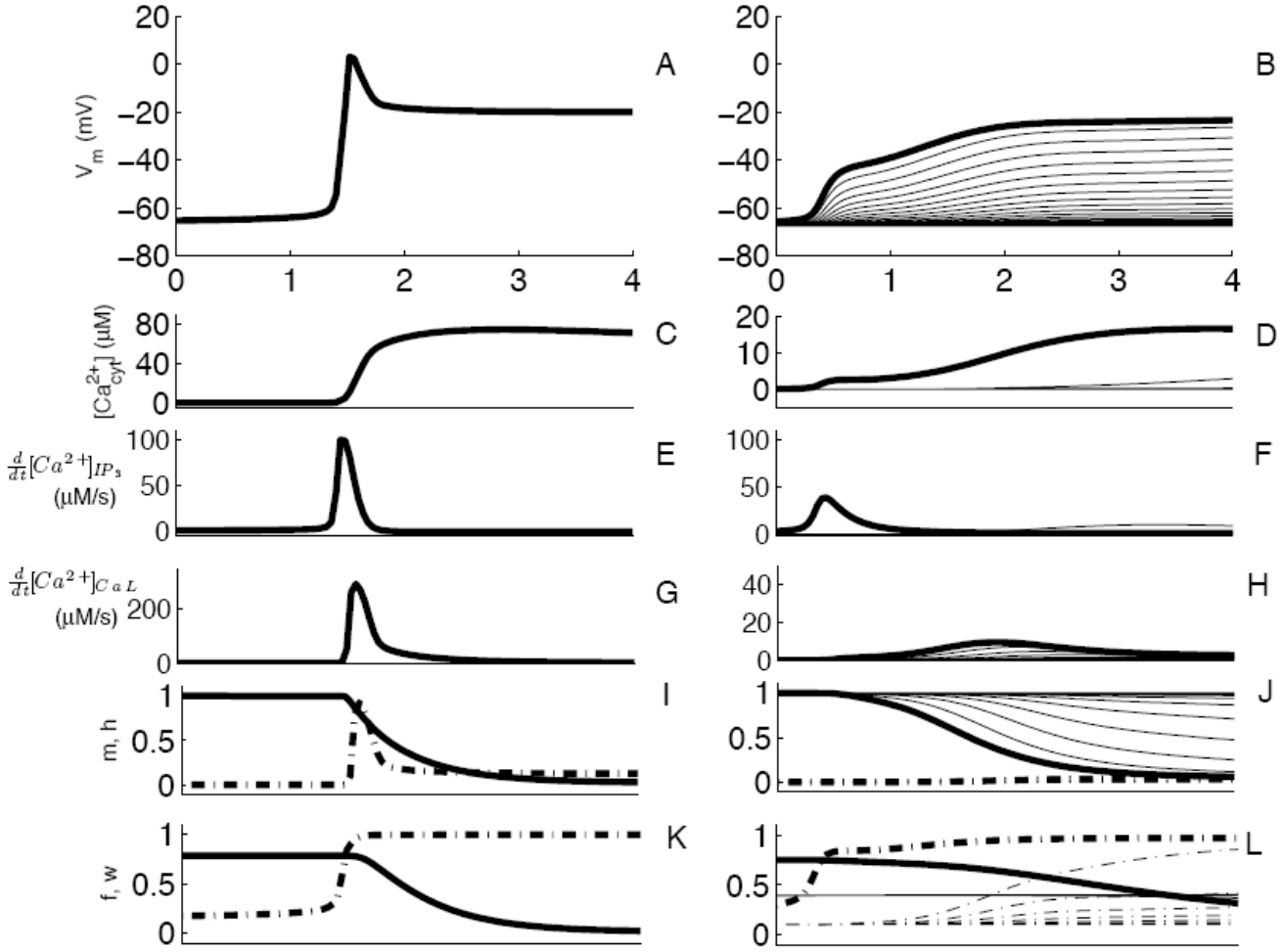
A
B
C
D
E
F
G
H
I
J
K
L
V_m (mV)
$[Ca^{2+}_{cyt}]$ (μM)
$\frac{d}{dt}[Ca^{2+}]_{IP_3}$ (μM/s)
$\frac{d}{dt}[Ca^{2+}]_{CaL}$ (μM/s)
m, h
f, w

Figure 5

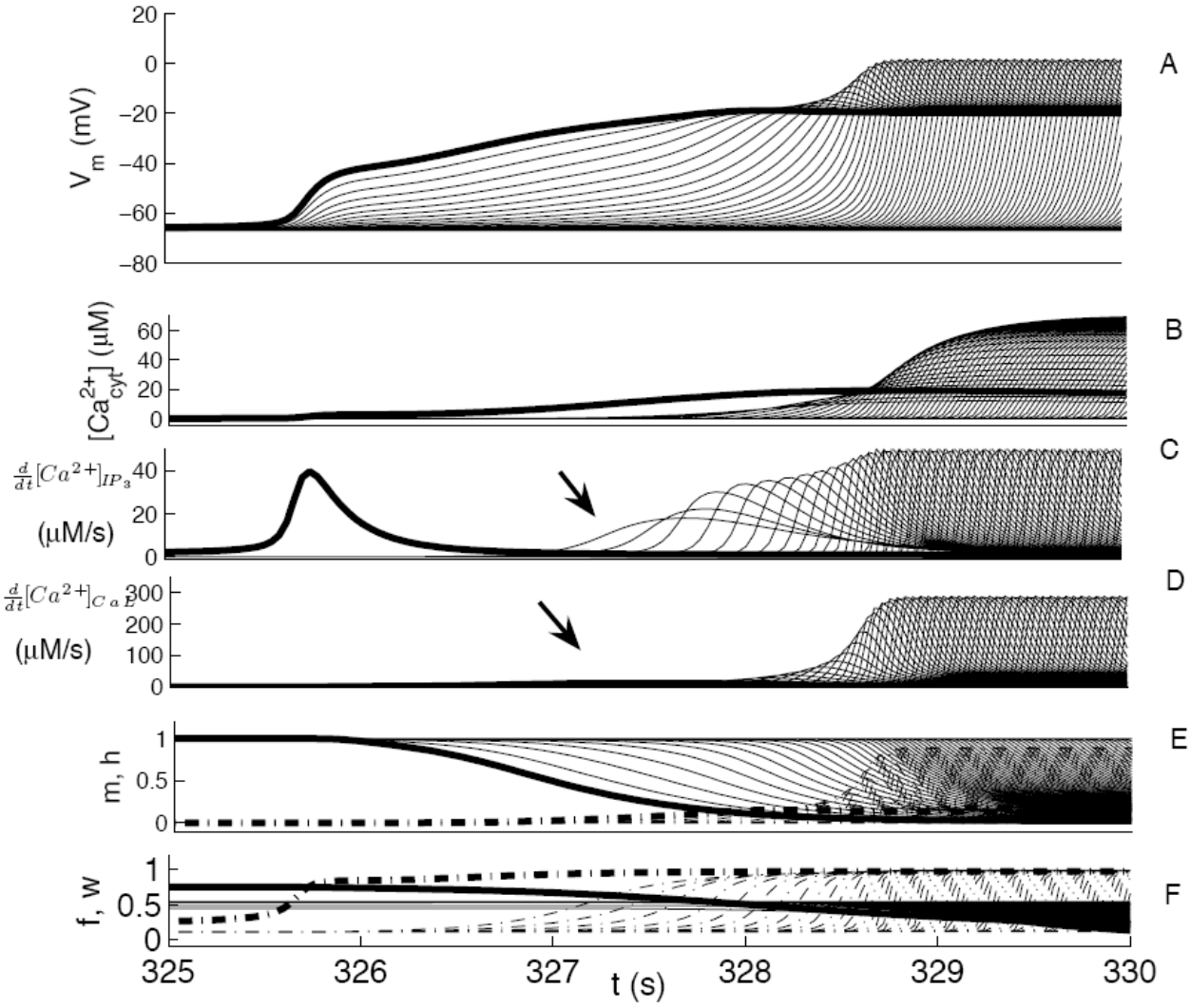
A
B
C
D
E
F
V_m (mV)
$[Ca^{2+}_{cyt}]$ (μM)
$\frac{d}{dt}[Ca^{2+}]_{IP_3}$ (μM/s)
$\frac{d}{dt}[Ca^{2+}]_{CaP}$ (μM/s)
m, h
f, w
t (s)

Figure 6

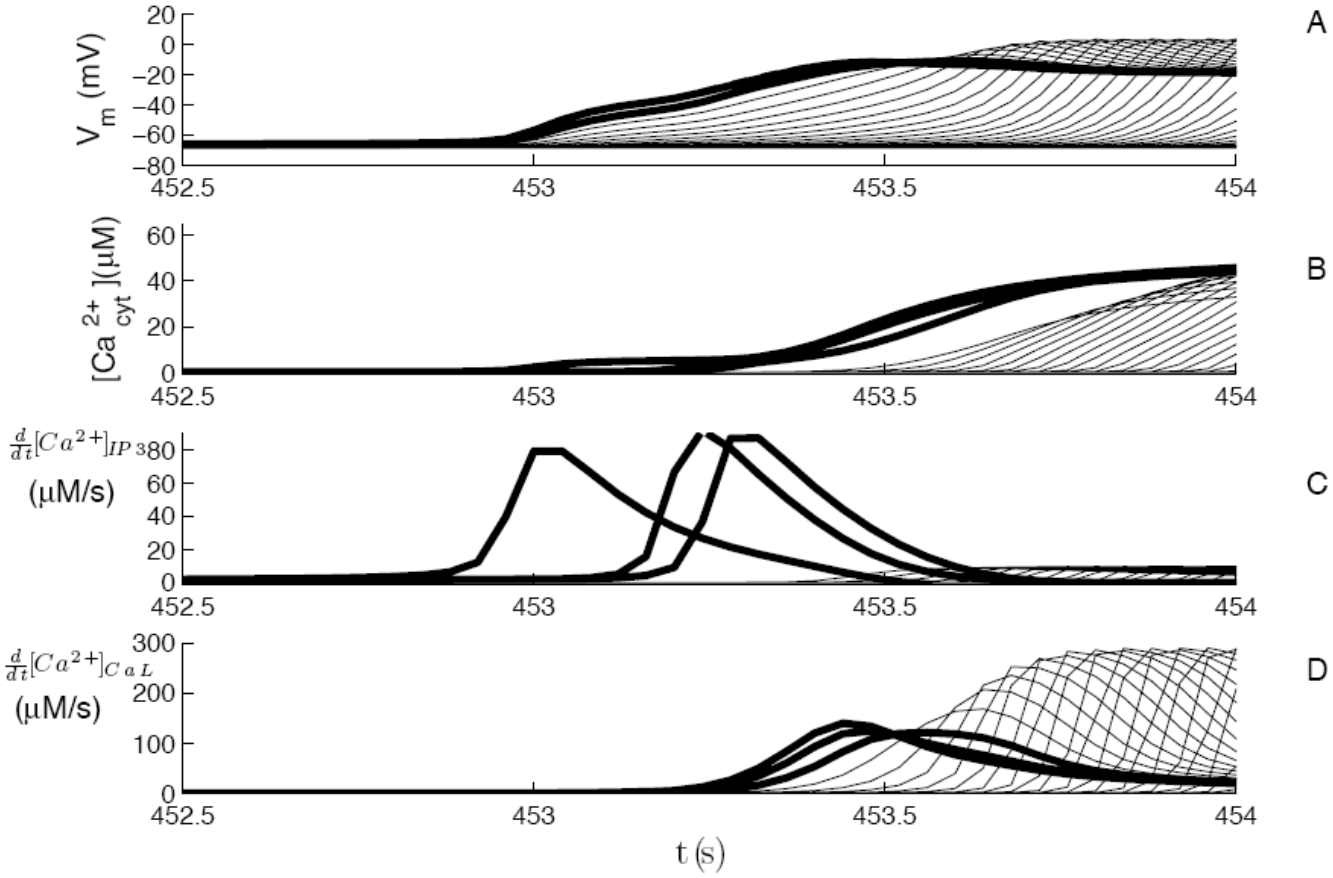
A
B
C
D
V_m (mV)
$[Ca^{2+}_{cyt}]$(μM)
$\frac{d}{dt}[Ca^{2+}]_{IP3}$ (μM/s)
$\frac{d}{dt}[Ca^{2+}]_{CaL}$ (μM/s)
20
0
−20
−40
−60
−80
60
40
20
0
80
300
200
100
452.5
453
453.5
454
t (s)

Figure 7

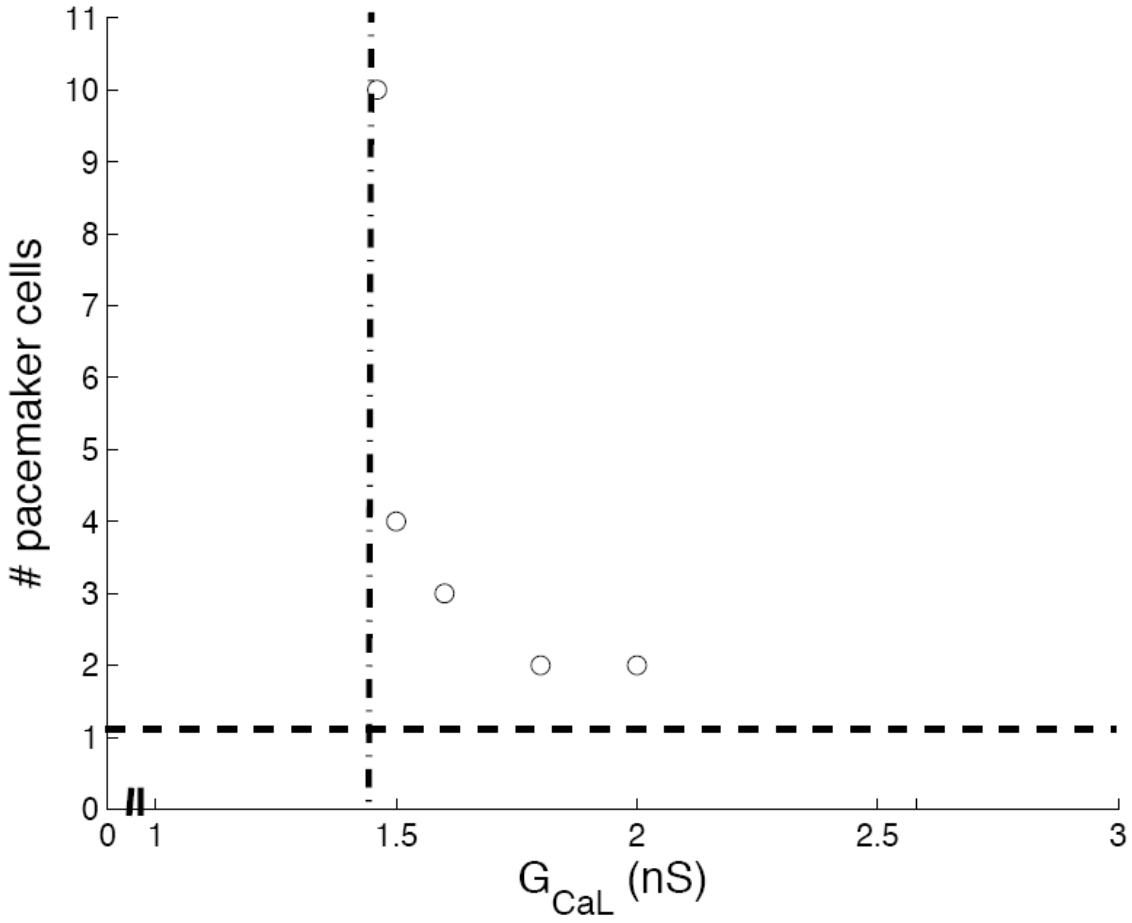

Figure 8

Table 1: Changed parameter values of the single-cell model.

$K_{Cl(Ca)}$	18	μM
G_{CaL}	1.6	nS
G_{lk}	0.058	nS
J_{PMCA}^{max}	3.0×10^{-5}	$\frac{\mu mol}{s \times dm^2}$
k_{on}	1.	$(\mu M s)^{-1}$
k_{off}	1.	s^{-1}
The membrane potential for half-maximal activation of m_∞	-10	mV